

# A Quantitative Analysis of the Dendritic Organization of Pyramidal Cells in the Rat Hippocampus

NORIO ISHIZUKA, W. MAXWELL COWAN, AND DAVID G. AMARAL

Department of Cell Biology, Tokyo Metropolitan Institute for Neuroscience, Tokyo, Japan (N.I.); Howard Hughes Medical Institute, Chevy Chase, MD (W.M.C.); Department of Psychiatry and Center for Neuroscience, University of California, Davis, California (D.G.A.)

## ABSTRACT

The three dimensional organization of the dendritic trees of pyramidal cells in the rat hippocampus was investigated using intracellular injection of horseradish peroxidase in the *in vitro* hippocampal slice preparation and computer-aided reconstruction. The total dendritic length, dendritic length in each of the hippocampal laminae, and the number of dendritic branches were measured in 20 CA1 pyramidal cells, 7 neurons in CA2 and 20 CA3 pyramidal cells. The total dendritic length of CA3 pyramidal cells varied in a consistent fashion depending on their position within the field. Cells located close to the dentate gyrus had the smallest dendritic trees which averaged 9,300  $\mu\text{m}$  in total length. Cells in the distal part of CA3 (near CA2) had the largest dendritic trees, averaging 15,800  $\mu\text{m}$ . The CA2 field contained cells which resembled CA3 pyramidal cells in most respects except for the absence of thorny excrescences on their proximal dendrites. There were also smaller pyramidal cells that resembled CA1 neurons. CA1 pyramidal cells tended to be more homogeneous. Pyramidal neurons throughout the transverse extent of CA1 had a total dendritic length on the order of 13,500  $\mu\text{m}$ . The quantitative analysis of the laminar distribution of dendrites demonstrated that the stratum oriens and stratum radiatum contained significant portions of the pyramidal cell dendritic trees. In CA3, for example, 42–51% of the total dendritic length was located in stratum oriens; about 34% of the dendritic tree was located in stratum radiatum. The amount of dendritic length in stratum lacunosum-moleculare of CA3 varied depending on the location of the cell. Many CA3 cells located within the limbs of the dentate gyrus, for example, had no dendrites extending into stratum lacunosum-moleculare whereas those located distally in CA3 had about the same percentage of their dendritic tree in stratum lacunosum-moleculare as in stratum radiatum. In CA1, nearly half of the dendritic length was located in stratum radiatum, 34% was in stratum oriens and 18% was in stratum lacunosum-moleculare. These studies identified distinctive dendritic branching patterns, in the stratum radiatum and stratum lacunosum-moleculare, which clearly distinguished CA3 from CA1 neurons.

© 1995 Wiley-Liss, Inc.

**Indexing terms:** CA3, CA2, CA1, dendrites, computer-aided morphometry

The three dimensional organization of a neuron's dendritic tree is an important determinant of its information processing capacity. The size and shape of the dendritic plexus clearly determines the types and numbers of inputs a particular neuron receives. Neuroanatomical attempts at defining these characteristics for the hippocampal pyramidal cells have taken place for more than a century. While Golgi (1886) conducted investigations of the hippocampus in a number of animal species, it was Ramón y Cajal (1901) who, using the Golgi technique, first clearly described differences in the size and shape of pyramidal cells in regio superior (CA1) and regio inferior (CA2/CA3) of the hippocampus. He noted that neurons in the regio inferior were

much larger than those in the regio superior and that the larger pyramidal cells were also distinguished by the presence of thorn-like excrescences on their proximal dendrite. He correctly surmised that these large, thorny spines were specialized for contact with the axons from the dentate gyrus. Lorente de Nò (1934) also used the Golgi method to further describe the dendritic and axonal morphology.

Accepted 11 April 1995.

Send correspondence and reprint requests to: Dr. David G. Amaral, Center for Neuroscience, University of California, Davis, 1544 Newton Ct., Davis, CA 95616.

hippocampal pyramidal cells. Among several important observations, he noted that the pyramidal cells of his CA2 region were as large as those in CA3 but lacked the excrescences characteristic of mossy fiber termination. While these classical studies established the foundations for much of our current thinking about the regional organization and intrinsic circuitry of the hippocampus, the observations were generally carried out in immature animals and were strictly qualitative. Thus, neither the three dimensional organization nor the quantitative features of mature hippocampal neurons were evaluated in these studies.

More recently, quantitative methods have been applied to the analysis of Golgi stained material from the developing and mature rat hippocampus (Minkowitz, 1976 a-c; Pokorny and Yamamoto, 1981; Fitch et al., 1989; McMullen et al., 1984). However, careful and systematic analysis of Golgi-stained material from the hippocampus (Desmond and Levy, 1982) has highlighted the fact that quantitative evaluation of this material is prone to a number of potential pitfalls. Impregnated neurons, for example, often have cut dendrites at the surface of the section. Unless corrected by serial reconstruction estimates, dendritic length measurements of such cells may seriously underestimate the total dendritic length of the neuron. Other technical problems, such as tissue shrinkage and the inherent capriciousness of the Golgi staining procedure, seriously compromise the effectiveness of this technique for providing reliable quantitative data.

Most recently, quantitative analysis of the organization of hippocampal neurons has turned to intracellular injection of tracer substances either *in vivo* (Sik et al., 1993; Li et al., 1994) or in the *in vitro* hippocampal slice preparation (Claiborne et al., 1990; Turner and Schwartzkroin, 1983; 1980; Trommald et al., 1995). These techniques, coupled with computer assisted analysis of the three dimensional organization of the dendritic tree, have provided unprecedented reliability in demonstrating the size and distribution of hippocampal cell dendrites. In a previous publication (Claiborne et al., 1990), we reported data on the dendritic trees of granule cells from the rat dentate gyrus that were intracellularly labeled in the *in vitro* slice preparation and subjected to computer assisted three dimensional reconstruction. This study demonstrated systematic variations

in the sizes and shapes of the granule cell dendritic trees depending on the location of the parent cell bodies. In the present study, we have used similar techniques to examine pyramidal cells of the CA3, CA2 and CA1 regions of the mature rat hippocampus. These studies demonstrate that the overall lengths of the dendritic trees of these neurons are substantially larger than previously appreciated and that the organization of pyramidal cell dendrites in the CA3/CA2 region is qualitatively different from that in CA1.

## MATERIALS AND METHODS

The methods used in this paper have been described in detail previously and will only be briefly reviewed here. The axons of some of the cells which are used for the present analysis have also been described previously (Ishizuka et al., 1990).

### Intracellular injection procedures

Sixty-five female, Sprague-Dawley rats (Zivic-Miller), ranging in age from 33 to 57 days old, were used in this study. The rats were anesthetized with ether, and decapitated. Each brain was quickly removed and immersed in ice-cold oxygenated saline for 15 seconds. After removing the hippocampus, 400 µm thick slices were cut perpendicular to the long axis of the hippocampus using a McIlwain tissue chopper. Slices from the middle third of the left hippocampus were placed on a filter membrane in a heated (32°C) slice chamber. Methods for maintaining the slices were similar to those described by others and in our previous reports (Claiborne et al., 1986; 1990; Ishizuka et al., 1990 and references therein). A standard interface chamber was used with fluid level adjusted so that the slice, which was supported by a micropore membrane, was just slightly submerged. Chamber fluid was exchanged approximately every 15–20 minutes. After a 1 hour recovery period, the temperature of the chamber was raised to 34°C before intracellular injection was attempted. Glass pipettes (70 and 80 Mohm) were filled with a solution of 2% HRP (Boehringer-Mannheim, Grade I) in 0.5M KCl/0.05M Tris buffer (pH 7.6) just prior to injection.

The slices were visualized through a Wild MP-5 stereomicroscope as the HRP-filled pipette was advanced in 4 µm steps into the pyramidal cell layer using a Burleigh piezoelectric microdrive. The impalement of a pyramidal cell was indicated by the sudden drop of the resting potential and the appearance of spontaneous discharges. If the resting potential of the impaled neuron remained stable at approximately -50 mV or less for 5 minutes and the amplitude of spontaneous activity was at least 50 mV, the intracellular injection was initiated. HRP was iontophoretically delivered using positive current pulses of 3 nA (250 ms duration, 2/s) for 15 to 24 minutes.

### Tissue processing

After allowing 2 to 7 hours for diffusion of the tracer, slices were fixed in a solution containing 1% paraformaldehyde and 2% glutaraldehyde in 0.1 M phosphate buffer (pH 7.3) for approximately 12 hours at 4°C. During early stages of this study, slices were fixed while stabilized between 2 sheets of filter paper. We found, however, that this procedure tended to flatten the slices and it was discontinued. Slices processed after the use of filter paper was discontinued averaged approximately 300 µm as judged from the Z axis of labeled dendrites (Tables 1–3). For visualization of

#### Abbreviations

CA1, CA2, CA3	Fields of the hippocampus
D	Distal portion of the CA3 field
DG	Dentate Gyrus
DGC	Granule cell of the dentate gyrus
EC	Entorhinal cortex
G	Granule cell layer of the dentate gyrus
H	Hilus of the dentate gyrus
M	Molecular layer of the dentate gyrus
Mid	Middle portion of the CA3 field
P	Proximal portion of the CA3 field
PCL	Pyramidal cell layer
PZ	Projection zone of stratum radiatum (CA3/CA2)
VD	Very distal portion of the CA3 field
hf	hippocampal fissure
ipb	infrapyramidal bundle of mossy fibers
l-m	stratum lacunosum-moleculare of the hippocampus
luc	stratum lucidum of the hippocampus
o	stratum oriens of the hippocampus
p	pyramidal cell layer of the hippocampus
r	stratum radiatum of the hippocampus
spb	suprapyramidal bundle of mossy fibers

TABLE I. Dendritic Parameters of CA3/CA2 Pyramidal Cells

Cell number	Location in CA3 (%)	Total dendritic length ( $\mu\text{m}$ )	ORI	Laminar dendritic length ( $\mu\text{m}$ )		Cell body area ( $\mu\text{m}^2$ )	Maximum length ( $\mu\text{m}$ )			Number of terminal branches (primary dendrite)	Cut dendritic branches
				LUC + P	RAD		X	Y	Z		
<b>CA3 Cells</b>											
A	C12973	5 P	7,569	4,308	674	2,587	0	297	320	410	294
B	C80764	8 P	9,942	4,532	526	4,884	0	280	459	601	283
C	C12877	9 P	11,122	2,747	992	6,994	389	428	710	661	276
D	C11471	16 P	8,637	4,607	856	3,070	104	351	579	643	249
E	C12873	17 P	9,037	2,205	921	4,999	912	407	626	769	46 (3)
F	C53063	18 P	8,868	4,032	667	3,987	181	340	427	637	311
G	C60463	19 P	9,830	4,818	438	3,539	1,015	246	341	648	237
H	C31162	32 M	11,488	4,995	320	4,675	1,498	501	320	791	266
I	C30573	36 M	12,460	5,562	467	4,886	1,485	319	377	810	346
J	C62563	35 M	12,581	5,990	125	3,728	2,739	381	491	776	245
K	C60361	46 M	11,369	4,876	179	4,478	1,836	455	376	668	247
L	C73164	52 M	11,552	5,025	245	4,555	1,727	437	316	856	332
M	C81463	56 M	13,889	6,492	258	4,796	2,943	435	346	778	323
N	C10861	74 D	15,243	8,152	438	3,661	3,002	750	390	941	222
O	C12866	75 D	17,492	8,424	460	5,409	3,199	714	427	590	39 (1)
P	C20467	78 D	15,931	7,599	482	4,848	3,002	586	397	968	240
Q	C40165	84 D	15,900	8,734	305	3,596	3,285	673	433	1,067	39 (1)
R	C82063	91 VD	17,928	7,224	666	5,558	4,480	502	425	1,003	36 (2)
S	C31164	92 VD	15,442	6,706	270	3,794	4,672	488	325	868	314
T	C73167B	94 VD	13,417	5,892	132	3,604	3,789	583	335	888	250
Mean $\pm$ S.D.				12,481.9 $\pm$ 2,998.9	5,645.5 $\pm$ 1,745.2	471.1 $\pm$ 250.2	4,382.4 $\pm$ 974.9	1,982.9 $\pm$ 1,458.0	458.7 $\pm$ 139.9	420.9 $\pm$ 105.5	786.0 $\pm$ 159.7
n = 20											39.7 $\pm$ 39.9
<b>CA2 Cells</b>											
U	C12979	CA2	16,205	5,194	96	5,921	4,994	640	315	938	347
V	C52061	CA2	16,403	6,572	22	4,924	4,385	624	395	921	316
W	C11571	CA2	14,083	5,766	109	3,963	4,246	391	336	887	253
X	C12971	CA2	14,932	5,929	56	4,386	4,561	409	411	857	323
n = 4	Mean $\pm$ S.D.	15,405.8 $\pm$ 949.7	5,865.3 $\pm$ 490.9	70.8 $\pm$ 34.3	4,798.5 $\pm$ 732.1	4,671.5 $\pm$ 292.8	516.0 $\pm$ 116.3	364.3 $\pm$ 39.9	900.5 $\pm$ 31.2	309.6 $\pm$ 34.7	51.8 $\pm$ 5.1
											40.5 $\pm$ 4.5

the HRP, the unsectioned slices were processed with 3,3'-5,5'diaminobenzidine (DAB). To promote penetration of reagents in order to insure that dendritic processes in the middle of the slice were well stained, slices were first incubated for 1 hour in a 1% solution of the detergent Triton X-100 in 0.1 M phosphate buffer, washed for 20 minutes in the same phosphate buffer and then preincubated in 0.05% DAB for 1 hour. The slices were then reacted for 30 minutes in the same concentration of DAB to which 0.01% H<sub>2</sub>O<sub>2</sub> was added. Following the DAB step, the slices were thoroughly washed, cleared in ascending concentrations of glycerol, mounted in 100% glycerol and cover-slipped. Glycerol was used as a clearing agent because earlier studies established that ethanol dehydration wrinkled and distorted the filled dendrites (Claiborne et al., 1986; Grace and Llinás, 1985).

### Analysis of filled neurons

Filled neurons were first photographed with a Leitz Dialux 20 microscope and then traced with the aid of a drawing tube using a 63X Zeiss Neofluar oil immersion objective with a 0.5 mm working distance. Dendrites and axons which were cut at the surfaces of the slice were noted on the drawings. The line drawing served as a check that all dendritic branches were included during the digitizing procedure. The computer microscope system has previously been described by Capowski and Sedivec (1981). Neurons were interactively digitized by an operator with each data point consisting of X, Y and Z (focal) coordinates. The digitized neuron could be reconstructed on a display screen, rotated in three dimensions, and printed as 2-dimensional hard copy on a digital plotter. Analysis software allowed various numeric and graphical representations of the dendritic trees.

While the decision to analyze labeled neurons in the unsectioned 400  $\mu\text{m}$  slice was beneficial for obtaining complete and accurate three dimensional reconstructions of the dendritic trees, it precluded other types of analyses. It was impossible, for example, to clearly resolve fine dendritic spines throughout the full thickness of the slice. No attempt was made, therefore, to carry out a quantitative analysis of the distribution or density of spines. Similarly, as neurons were digitized, the diameter of plotted dendrites was entered into the computer along with the three dimensional coordinates of data points. Taken together, this provided the necessary information to develop estimates of the surface area and volume of labeled neurons. These estimates must be considered rather rough approximations, however, for the following reasons. First, the diameters of the finest distal dendrites of the pyramidal cells approached the limit of the light microscope ( $\approx 0.25 \mu\text{m}$ ) and these were particularly difficult to resolve and accurately determine their diameter when they occurred deep in the slice. Second, the computer-aided tracing system did not provide the capability of assigning dendritic diameters smaller than 0.3  $\mu\text{m}$ . Thus, all dendritic branches thinner than 0.3  $\mu\text{m}$  were logged in with a diameter of 0.3  $\mu\text{m}$ . This likely inflated the volume estimates somewhat and we will discuss this in more detail at the appropriate point in the Results. While the thickness data are typically not presented in our illustrations of filled neurons (for example in Figure 8), Eutectics Neuron Tracing System computer files which include thickness measurements are available for all neurons evaluated in this study to any interested investigator.

## RESULTS

### Selection of pyramidal cells for analysis

In the hippocampal slices prepared for this study, intracellular injections were attempted in 210 neurons throughout CA1, CA2 and CA3. Of these, 109 cells demonstrated HRP reaction product. From this population, a group of 47 cells was selected for quantitative analysis. Twenty of these cells were located in CA3, 7 were located in the CA2 region and 20 were injected in CA1. While all of the 109 labeled cells demonstrated some portion of their dendritic tree, several had one or more cut dendrites at the surface of the slice. Other labeled neurons had only faint labeling which apparently did not extend to the tips of the dendrites. The selected neurons had dark and homogeneous labeling of all components of the dendritic trees. This labeling clearly extended to the finest distal tips of the dendrites that could be resolved with the light microscope. Labeled neurons with clear transections of a thick, proximally situated dendrite were excluded from further analysis. Many of the neurons that were selected for analysis had no perceptible cut dendritic segments (Tables 1 and 2). Some neurons with cut dendrites were accepted for analysis, however, if it was clear that the cut dendrites were terminal branches of the dendritic tree and thus contributed relatively little to the total dendritic length.

### Nomenclature

We have previously reviewed the nomenclature historically applied to the hippocampus of the rat (Ishizuka et al., 1990). In that paper, as in this one, we use the nomenclature suggested by Lorente de Nó (1934). Thus, the hippocampus proper is divided into three fields, CA1, CA2, and CA3. Lorente de Nó (1934) further partitioned the CA3 and CA1 fields based largely on the dendritic and axonal appearance of neurons in his Golgi preparations. He divided field CA3 into three subfields, field CA3c located closest to the dentate gyrus, CA3b in the mid region of CA3, and CA3a at the border with CA2. Lorente de Nó (1934) indicated that the criteria for partitioning the CA3 field were not definitive and many of the distinctive features were only visible in Golgi stained material. In the present study, we have noted a gradual change in the appearance of CA3 pyramidal cells as their locations move from proximal (close to the dentate gyrus) to distal (close to CA2). The population of CA3 cells that we have examined do not provide strong evidence for Lorente de Nó's subdivision of the CA3 field into 3 distinct parts. We have decided, therefore, to use a proximodistal nomenclature to describe the position of the labeled cells within the field. Cells located close to the dentate gyrus are considered to be proximal and those close to the CA2 field are distal. It will prove useful, however, to discuss the common features of pyramidal cells in certain portions of the CA3 region and for this purpose we will describe neurons as located in proximal, mid, distal and very distal portions of the CA3 field. The proximal portion is that part of CA3 that is enclosed within the limbs of the dentate gyrus and is further characterized by the presence of an infrapyramidal bundle of mossy fibers. The distal portion of CA3 is defined as that part that lies directly superficial to the fimbria. The mid portion lies between the proximal and distal portions and the very distal portion lies between the distal CA3 and CA2. As in our previous study (Ishizuka et

TABLE 2. Dendritic Parameters of CA1 Pyramidal Cells

Cell number	Location in CA1 (%)	Total dendritic length (μm)	Laminar dendritic length (μm)			Cell body area (μm <sup>2</sup> )	Maximum length (μm)			Number of terminal branches (primary dendrite)			
			ORI	RAD	MOL		X	Y	Z	Apical	Basal	Cut dendritic branches	
a C91665	1	12,335	3,660	6,610	2,075	243	484	1,105	360	62 (1)	22 (1)	2	
b C73166A	1	15,509	4,894	7,530	3,085	230	329	904	291	87 (3)	41 (4)	12	
c C73166B	1	13,963	4,225	5,513	4,225	244	340	911	260	72 (2)	30 (2)	1	
d C81462	15	11,895	4,431	5,074	2,390	178	406	885	261	53 (1)	27 (5)	0	
e C30465	22	12,818	4,034	6,389	2,415	124	346	989	262	65 (1)	26 (3)	0	
f C9286E	24	14,191	5,244	6,516	2,431	197	562	904	242	57 (1)	32 (4)	0	
g C70863	24	12,909	4,577	6,485	1,847	130	448	903	301	59 (2)	28 (4)	0	
h C80761	25	11,127	3,092	5,637	2,398	180	343	848	263	57 (1)	21 (4)	0	
i C8076E	25	14,100	6,589	5,551	1,960	170	373	892	313	50 (1)	41 (5)	1	
j C91662	29	14,771	4,805	7,243	2,723	206	495	935	287	68 (2)	30 (2)	1	
k C72865	31	12,605	5,115	5,366	2,124	186	438	778	193	60 (1)	36 (4)	3	
l C73162	33	13,392	1,884	8,971	2,537	150	444	886	287	87 (3)	12 (1)	2	
m C20465	37	13,710	5,184	5,630	2,896	113	448	952	276	50 (1)	37 (5)	0	
n C62564	37	12,782	5,439	5,673	1,670	175	390	940	48 (1)	32 (3)	0		
o C20466	37	14,440	3,783	7,674	2,983	228	404	837	244	77 (2)	24 (4)	1	
p CD1152	37	11,946	3,970	6,328	1,648	226	406	909	137	58 (2)	21 (2)	3	
q C11563	37	13,215	5,014	6,017	2,184	98	463	968	247	55 (1)	33 (4)	1	
r C12861	40	14,316	5,407	5,707	3,202	245	494	907	281	61 (1)	32 (4)	1	
s C70863	40	12,595	5,136	5,115	2,344	155	404	869	303	54 (1)	32 (3)	4	
t C12862	47	14,472	5,463	6,169	2,840	194	452	925	256	59 (1)	35 (4)	0	
u CD2351	54	14,041	4,034	7,576	2,431	204	432	927	210	75 (1)	24 (2)	0	
v CD0351	58	14,644	4,867	6,871	3,106	282	545	1,166	240	49 (2)	30 (3)	1	
w C10261	66	12,980	4,826	5,434	2,720	280	386	803	207	55 (1)	30 (4)	0	
n = 23		Mean ± S.D.	13,424.2 ± 1,060.9	4,585.8 ± 934.9	6,306.5 ± 570.5	193.0 ± 49.3	428.2 ± 61.7	919.1 ± 74.0	259.6 ± 40.0	61.7 ± 11.2	29.4 ± 6.6		

These cells were located deep to the CA2 pyramidal layer.

TABLE 3. Relationship Between Numbers of Apical Dendrites and Dendritic Parameters

Number of primary apical dendrites	Statistical analysis					
	1	2	3	1 vs. 2	1 vs. 3	2 vs. 3
Number of cells	15	6	2			
Total dendritic length ( $\mu\text{m}$ )	$13,146 \pm 948$	$13,779 \pm 1,024$	$14,451 \pm 1,059$	ns	ns	ns
Total apical dendritic length ( $\mu\text{m}$ )	$8,301 \pm 745$	$9,441 \pm 958$	$11,062 \pm 447$	*	**	ns
Total basal dendritic length ( $\mu\text{m}$ )	$4,845 \pm 837$	$4,338 \pm 374$	$3,389 \pm 1,505$	ns	ns	ns
Number of terminal apical branches	$57.4 \pm 6.6$	$63.8 \pm 9.4$	87.0	ns	**	*
Number of terminal basal branches	$30.7 \pm 5.5$	$27.2 \pm 3.5$	$27.5 \pm 9.1$	ns	ns	ns

\* $P < 0.05$ . Two-tailed student's *t* test.

\*\* $P < 0.001$ .

al., 1990), we have identified a small portion of the hippocampal pyramidal cell layer as CA2. As we will describe, this tends to be a heterogeneous region with overlapping elements from CA1 and CA3. There is, however, a distinct class of CA2 pyramidal cells that presumably give rise to the distinctive axonal projections that we described previously (Ishizuka et al., 1990—this paper should be consulted for a more detailed description of CA2).

Although Lorente de Nô (1934) also divided the CA1 field into three parts (CA1a, CA1b and CA1c), we found no distinctions in the morphology of the CA1 pyramidal cells that would allow such a subdivision. When describing CA1 pyramidal cells in different portions of the field, we will employ a proximodistal terminology similar to that described for CA3. Thus, the portion of CA1 closest to CA2 is defined as proximal and that closest to the subiculum as distal. It should be noted that since the very distal portion of the CA1 pyramidal cell layer overlaps the proximal portion of the subiculum, and the pyramidal layers become difficult to discriminate in the *in vitro* slice preparation, we have not attempted to label neurons in this region.

The CA fields of the hippocampus are generally subdivided into several laminae. From the ventricular to the pial surfaces these include: the alveus; stratum oriens; the pyramidal cell layer; stratum lucidum (the mossy fiber layer found only in CA3); stratum radiatum and stratum lacunosum-moleculare. In describing the radial organization of the pyramidal cell dendritic trees, those dendrites located closer to the hippocampal fissure are described as superficial and those located closer to the alveus as deep.

For reasons that will become clearer below, we have operationally subdivided stratum radiatum of the CA3 region into a superficial fifth that we will refer to as the **projection zone**, and the deeper four fifths that we will refer to as the **associational zone**. We have found that the projection zone is the region in which fibers from proximal CA3 travel to the distal portion of CA1 (Ishizuka et al., 1990). Axons in this region are thick and bear few varicosities. As we will describe in some detail, the dendrites of CA3 pyramidal neurons that travel through the projection zone have few side branches. This is in striking contrast to the situation in the associational zone of stratum radiatum where numerous dendritic side branches are observed (see below). These observations have led us to conclude that

most of the associational connections of the CA3 cells are established in the deep four fifths of stratum radiatum and that the superficial fifth is primarily a region of axonal passage.

### General appearance of hippocampal pyramidal cells

The only general description of the pyramidal cells of the rodent hippocampal formation has been provided by Lorente de Nô (1934). His descriptions were based on the analysis of Golgi preparations obtained from young animals. While many of the observations from our intracellular preparations are consistent with his findings, there are also a number of features of the neurons that we have labeled that are at variance with his description. We shall begin with a brief overview of the general appearance of pyramidal cells in the CA3, CA2 and CA1 hippocampal fields followed by a more detailed description of the cells in each of these fields.

The cell bodies of pyramidal cells in CA3 and CA2 were of approximately the same size and their cross sectional surface areas were approximately 2–3 times that of the cells in CA1 (Tables 1 and 2; Figs. 13 and 15). All hippocampal pyramidal cells had prominent apical and basal dendritic trees (Figs. 1–5, 11, 12 and 15). In CA3 and CA2, there were 1–3 primary apical dendrites originating from the soma that often branched to produce 4 or more thick, secondary apical dendrites (Figs. 1–5, 8). Primary dendrites were those that originated from the soma and secondary dendrites were those thick dendrites that branched from the primary dendrites. The secondary branches gave rise to thinner, higher order dendritic branches that we generally refer to as side branches. In CA1, there was typically only 1 or 2 primary apical dendrites which did not divide further along their ascent towards stratum lacunosum-moleculare (Figs. 8, 11, and 12). In CA3 and CA2, there were between 2 and 7 primary basal dendrites and in CA1 there were between 1 and 5 primary basal dendrites (Tables 1 and 2).

One area in which our findings disagree with those of Lorente de Nô (1934) concerns the organization of dendritic branches in stratum radiatum. He suggested that while CA1 pyramidal cells demonstrated numerous side branches in stratum radiatum, those in CA2 and CA3 were devoid of these branches. A survey of Figures 1–5, 11 and 12 demonstrates, however, that in the rat, dendritic side branches in stratum radiatum are as common in CA3 and CA2 as in CA1. These side branches, however, were organized somewhat differently in CA1 than in CA2 and CA3. In CA3 and CA2, side branches were confined to the deep four fifths of stratum radiatum and tended to leave the secondary dendrites at oblique angles i.e. nearly perpendicular to the primary apical dendrite (Figs. 1–5). There were few, if any, side branches in the projection zone, which occupies the superficial one fifth of stratum radiatum of CA3 and CA2. In CA1, in contrast, dendritic side branches occurred throughout the full radial extent of stratum radiatum (Figs. 11 and 12). In the deep portion of the layer, the side branches were obliquely oriented as in CA3. But in the superficial portion of stratum radiatum the side branches tended to have a more acute or radial angle of departure from the secondary dendrites (cf Figures 3 and 11).

The distal dendrites located in stratum lacunosum-moleculare were also organized in a distinct fashion in CA3/CA2 versus CA1. In CA3/CA2, the distal apical den-

drites were oriented mainly vertically and their width did not usually exceed the width of dendrites in stratum radiatum or stratum oriens (Table 1; Figs. 1–6). In CA1, however, the distal dendrites tended to run transversely for some distance beneath the hippocampal fissure. The dendritic plexus of CA1 pyramidal cells in stratum lacunosum-moleculare, therefore, was often substantially wider than in stratum radiatum or stratum oriens (Figs. 6, 11 and 12).

### General appearance of spines on hippocampal pyramidal cells

While we have not conducted a quantitative analysis of the distribution of dendritic spines on hippocampal pyramidal cells, as illustrated in Figures 1–4 and 11, there were qualitative differences in the spacing of spines on different portions of the dendritic tree (Figs. 13 and 14). The primary dendrites tended to show fewer typical spines than on the secondary and higher-order, thinner dendritic branches. The proximal portions of CA3 apical dendrites that traveled through stratum lucidum, where the specialized mossy fiber thorny excrescences are present, demonstrated few, if any, classical spines. Spines located on the dendritic branches in stratum oriens and stratum radiatum appeared to be similar in size, shape and spacing. Spines in stratum lacunosum-moleculare, however, appeared to be spaced at substantially greater distances on the dendrites. We shall now return to a more detailed exposition of labeled cells in CA3, CA2 and CA1 of the hippocampus.

### Dendritic organization of CA3 pyramidal cells

Perhaps the most interesting feature of the organization of CA3 pyramidal dendritic trees is their systematic variation both of total dendritic length and of the proportion of dendritic tree in the various layers of the hippocampus as a function of the proximodistal location of the cell body. Cells located proximally in CA3 had the smallest total dendritic length and cells located distally had the longest dendritic length (Table 1; Figs. 5, 9 and 15). Interestingly, there was also a range in the somal size of the pyramidal cells with the smallest cell bodies generally located proximally in the field (Table 1). As illustrated in Figure 10A, there was a clear relationship between the cross sectional area of CA3 cell bodies and their total dendritic length; the larger the cell body, the longer the total dendritic length. There was also a positive correlation between the total number of terminal dendritic branches and the total dendritic length of CA3 cells (Fig. 10B).

As described in the Materials and Methods, we analyzed the amount of dendritic tree in each lamina of the hippocampus. The amount of dendritic tree located in the major layers of the hippocampus in different portions of CA3 is plotted in Figure 9. The length of dendrite for each CA3 neuron in each of the hippocampal laminae is also listed in Table 1. The following conclusions can be drawn from these data.

In stratum oriens, the total length of the basal dendrites was greatest in the distal portion of the field (Fig. 9). In this portion of CA3, the basal dendrites accounted for approximately 51% of the total dendritic length. In other portions of CA3, the basal dendrites accounted for approximately 42–45% of the total dendritic tree. A relatively small amount of dendrite was contained within the pyramidal cell layer or within stratum lucidum. In the proximal portion of CA3, there is both a suprapyramidal bundle of mossy fibers and an infrapyramidal bundle. As noted above, throughout

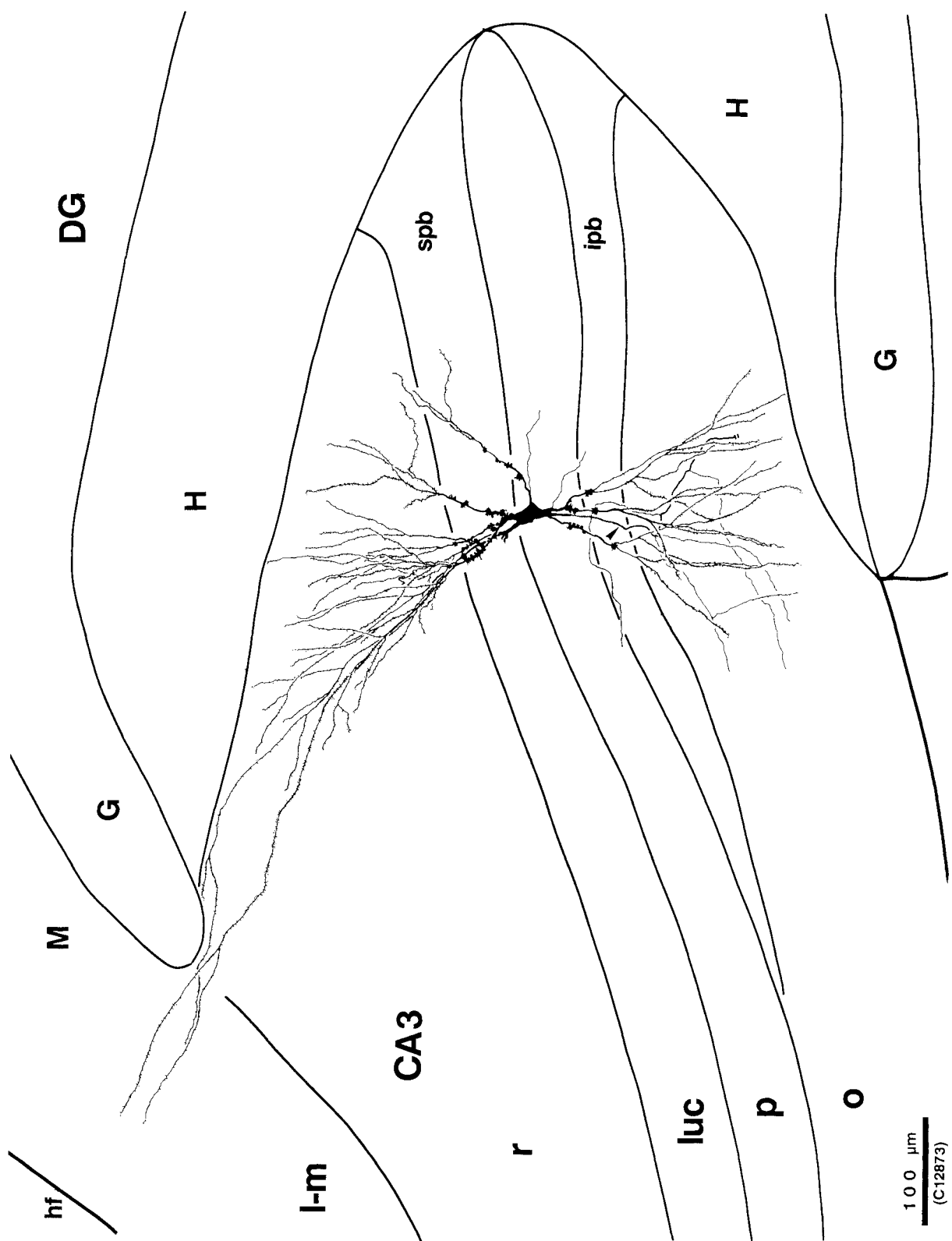
CA3 the proximal dendrites that pass through stratum lucidum have few, if any, standard spines but contain the large, thorny excrescences characteristic of mossy fiber termination (Figs. 1–3; 13 C and D). In the proximal part of the field, the basal dendrites passing through the infrapyramidal bundle of mossy fibers have the same features as the apical proximal dendrites. In the measurements shown in Table 1, the dendritic length reported for the pyramidal cell layer and stratum lucidum comprise all of the dendrites in both the infra- and suprapyramidal mossy fiber bundles. This accounts for the somewhat higher amount of dendritic tree in these zones on cells located in the proximal portion of the field. In the mid and distal portions of the CA3 field, the infrapyramidal bundle of mossy fibers could not be detected in our preparations. However, there were occasional thorny excrescences on the proximal basal dendrites of pyramidal cells in these parts of CA3 (Figs. 2 and 13d). Occasional mossy fiber varicosities are normally observed in this portion of the CA3 pyramidal cell layer (Amaral and Dent, 1981; West et al., 1981).

The organization of dendrites in stratum radiatum is quite distinctive. As noted above, the bulk of the dendritic tree in this layer is located in the deep four fifths of the layer (Figs. 2–5). In the superficial fifth of the layer, there is very little branching from the secondary dendrites and branching does not recommence until the dendrites reach stratum lacunosum-moleculare. In our previous paper on the connections of CA3 pyramidal cells (Ishizuka et al., 1990), we noted that axonal fibers located in the superficial fifth of stratum radiatum in CA3 were relatively thick and contained few varicosities. The characteristics of the axons in this region led us to speculate that most of the CA3 to CA3 associational connections occurred in the deep four fifths of stratum radiatum where axonal collaterals tended to be thinner and highly varicose. The finding that the bulk of dendritic branching occurs in the associational zone of stratum radiatum is consistent with that interpretation.

The summed dendritic length of dendrites in stratum radiatum was relatively constant in all transverse portions of CA3 (Fig. 9). As a proportion of the total dendritic length, however, the stratum radiatum dendrites contributed most to the dendritic trees of cells in the proximal portion of the field. Here, there was approximately 46% of the dendritic tree in stratum radiatum. The lowest proportion of dendrites in stratum radiatum (27%) was observed in the distal portion of CA3.

The amount of dendritic tree located in stratum lacunosum-moleculare varied substantially depending on the proximodistal location of the pyramidal cell. The CA3 pyramidal cells located proximally in the field had little or no dendritic tree in stratum lacunosum-moleculare (Table 1; Fig. 9). Beyond this portion, however, there was an increasing gradient both of total dendritic length in stratum lacunosum-moleculare and of the percentage of total dendritic tree in this layer. The percentage of total dendritic length in stratum lacunosum-moleculare was 4% in proximal cells, 16% in middle cells, 19% in distal cells and 28% in the very distal cells.

As indicated in Table 1, the mean transverse extent of the CA3 pyramidal cell dendritic tree was approximately 400  $\mu\text{m}$  (X in Table 1). The mean septotemporal extent of the dendritic tree, in the thickness of the slice, was approximately 300  $\mu\text{m}$  (Z in Table 1). The generally similar dimensions of the dendritic trees in the septotemporal and



Note also that the large thorny excrescences characteristic of mossy fiber termination (black irregular regions on proximal dendrites) are located both on apical and basal proximal dendrites of this neuron. The axon of this neuron is indicated with an arrowhead and the cut end of the secondary apical dendrites extend around the suprapyramidal blade

Fig. 1. Camera lucida drawing of a CA3 pyramidal cell located in the proximal portion of the CA3 field. Note that the apical dendrites of this neuron do not enter the hilus (H) of the dentate gyrus. At least some of the secondary apical dendrites extend around the suprapyramidal blade

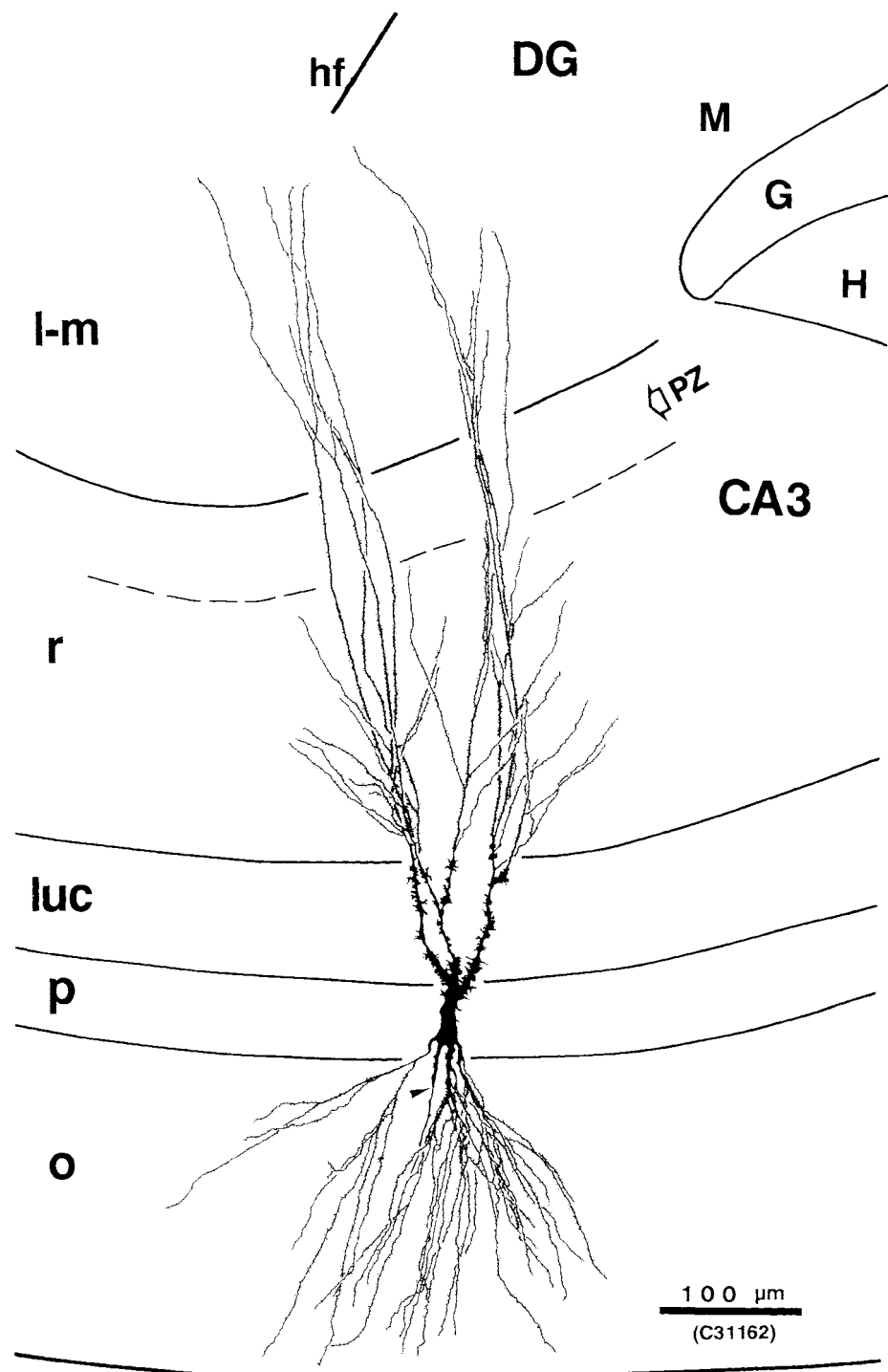


Fig. 2. Camera lucida drawing of a CA3 pyramidal cell located in the middle portion of the field. As this neuron lies outside of the zone of the infrapyramidal mossy fiber bundle, most of the thorny excrescences are located on the proximal apical dendrites. Note that dendritic side

branches occur in the deep four fifths of stratum radiatum but do not enter the projection zone (PZ). The axon of this neuron is indicated with an arrowhead.

transverse axes can be appreciated in Figure 6 where the computer generated plot of a CA3 neuron has been rotated 90° (side) from the transverse plane. The mean height of the CA3 cells was approximately 800 µm (Y in Table 1). The

height of the CA3 cells also varied substantially depending on their proximodistal location. Proximal neurons were as short as 400 µm whereas some distal neurons were more than 1 mm in height.

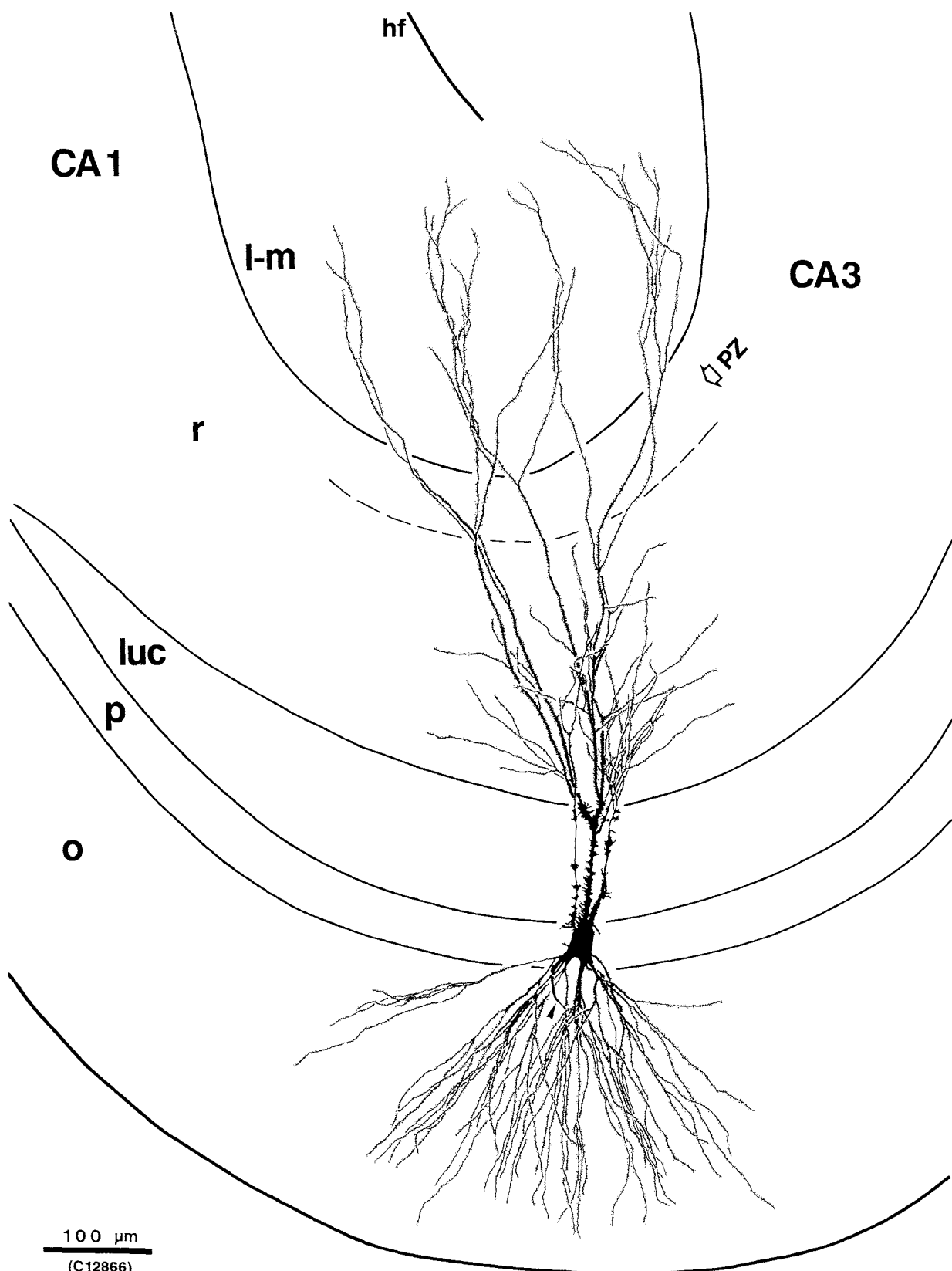


Fig. 3. Camera lucida drawing of a CA3 neuron in the distal portion of the field. Virtually all of the dendritic side branches in stratum radiatum are located in the deeper portions of stratum radiatum and there are few of these branches in the projection zone (PZ) indicated by a dashed line and open arrowhead. Branching of the dendritic tree

recommences once the dendrites enter stratum lacunosum-moleculare (l-m). Large numbers of thorny excrescences are seen on the proximal apical dendrites of this neuron; there are few typical spines, however, in the region of stratum lucidum. The axon of this neuron is marked with an arrowhead.

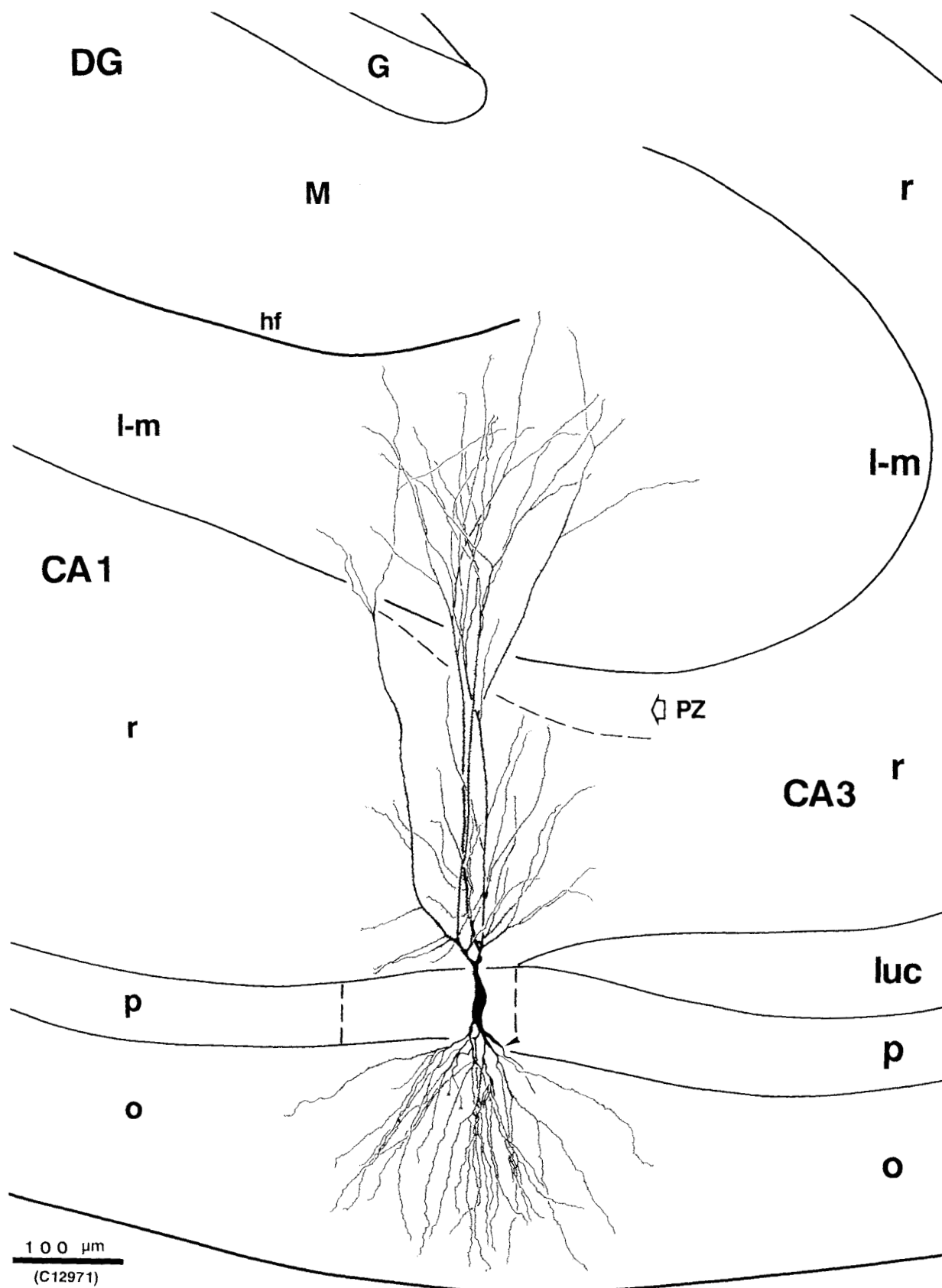


Fig. 4. Camera lucida drawing of a CA2 neuron. Note that while the size and general dendritic characteristics of this neurons are similar to those in CA3, there are no thorny excrescences on the proximal apical dendrites. As with the CA3 neurons, most of the dendritic side branches in stratum radiatum are located in the deeper four fifths of the layer.

The projection zone is decreasing in thickness as it approaches CA1. The axon of this neuron is indicated with an arrowhead. Two basal dendrites cut at the surface of the slice are indicated by asterisks. Dashed lines in the pyramidal cell layer indicate the approximate boundaries of the CA2 field.

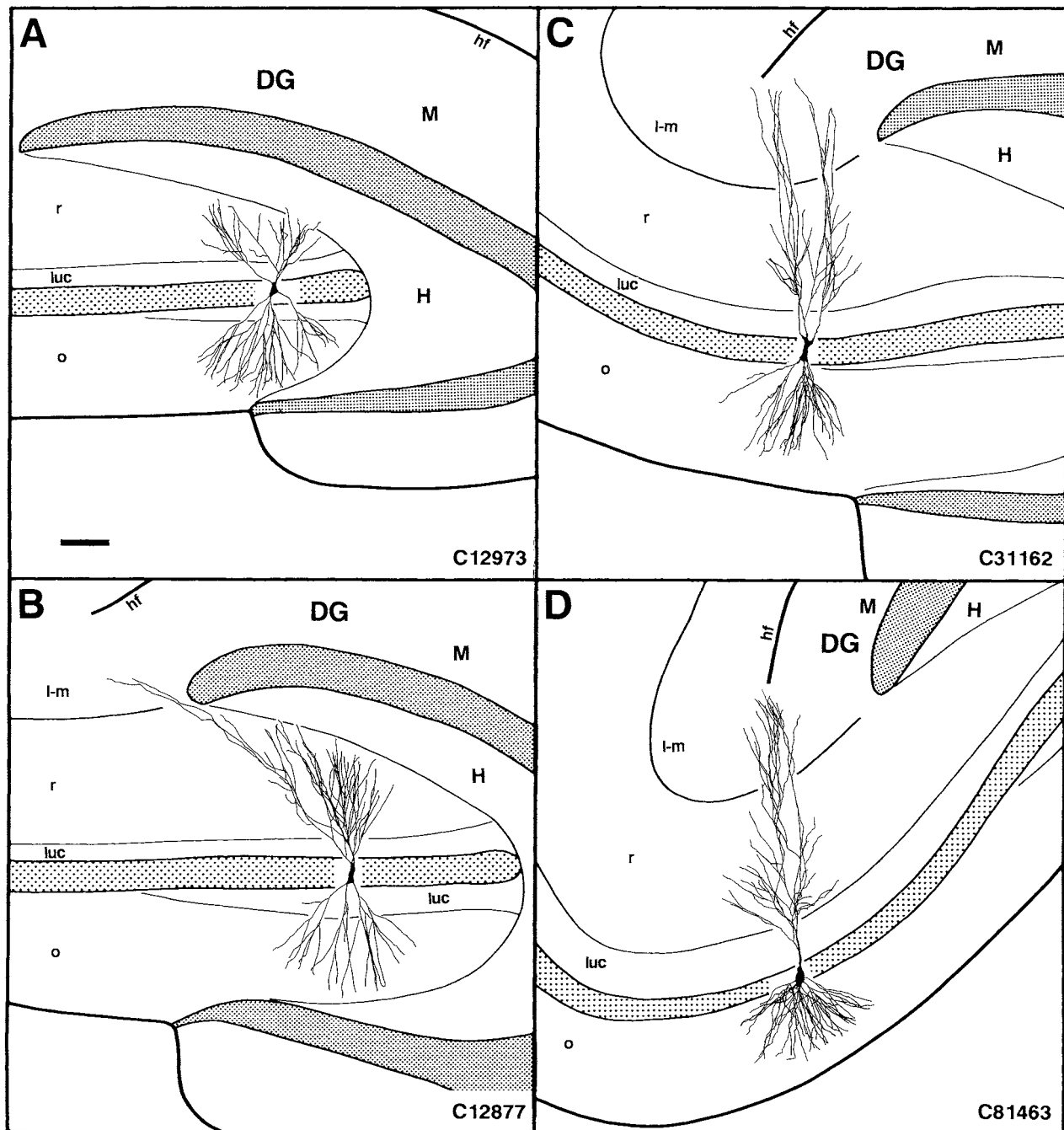


Fig. 5 (A–H). Computer generated line drawings of CA3 pyramidal cells in positions ranging from proximal (A) to very distal (H) in the field. See text for details. Shaded areas indicate granule cell and pyramidal cell layers. Neither the thorny excrescences on the proximal

CA3 dendrites nor the more typical spines on the more distal dendrites are indicated on these computer generated line drawings. Scale bar: 100  $\mu\text{m}$ .

As noted in the Methods section, the diameter of dendrites was entered during the three dimensional digitization process and thus an estimate of the cell volume could be generated. It should be noted, however, that since we did not quantify the number of dendritic spines and have not included their surface area or volume in the estimates below, these estimates must be considered only approximate. As with the other parameters of CA3 cell morphology,

the volume of neuronal dendritic trees varied substantially along the transverse axis of the field. Cells located proximally had the smallest average volume which was on the order of  $2,144 \mu\text{m}^3$ . Cells located in the mid region of CA3 had an average volume of  $3,681 \mu\text{m}^3$ . Cells located distally in CA3 had an average volume of  $3,194 \mu\text{m}^3$  and very distal CA3 neurons had an average volume of  $5,412 \mu\text{m}^3$ . CA2 neurons had an average volume of  $5,920 \mu\text{m}^3$ . Due to the

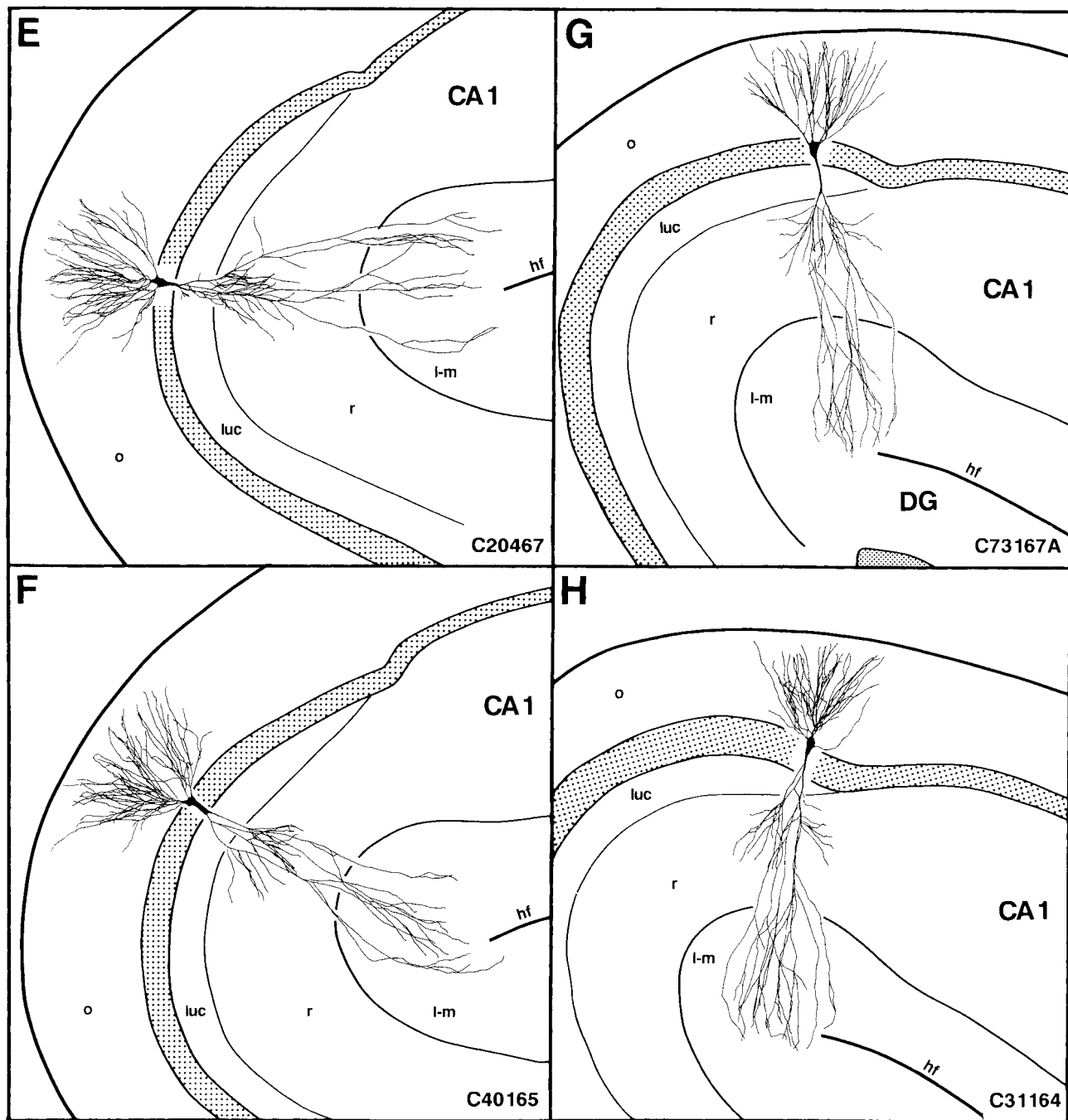


Figure 5 (Continued.)

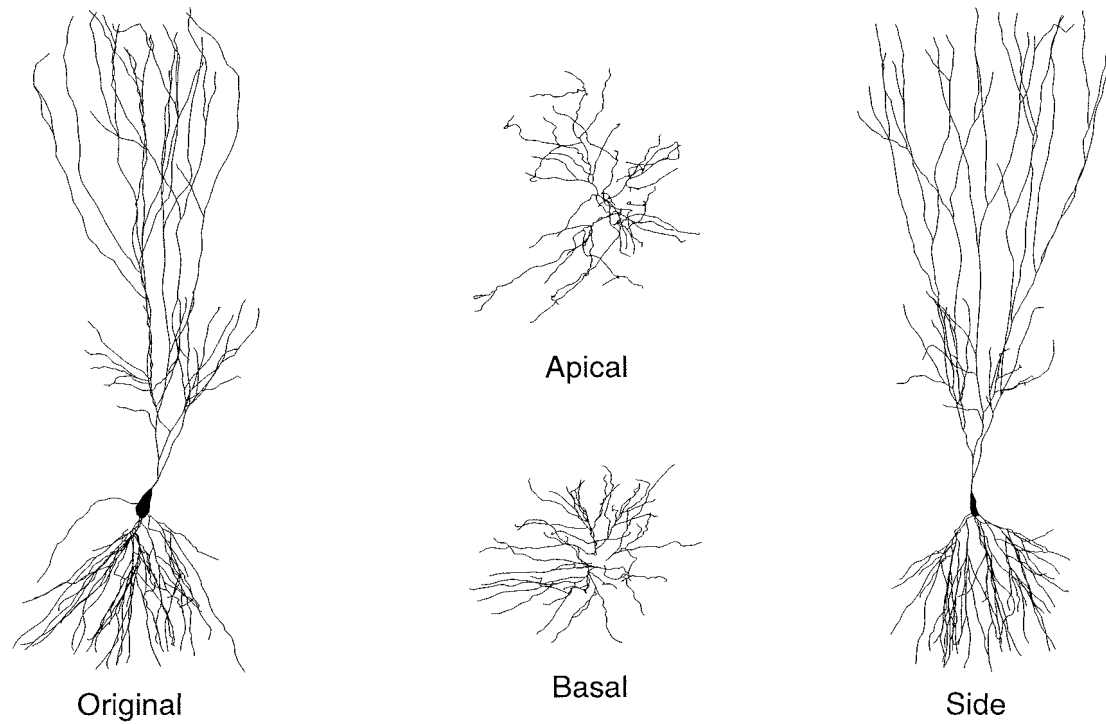
analysis system limitation of entering the finest dendrites with a diameter of 0.3  $\mu\text{m}$  diameter, these numbers may overestimate the true volume somewhat. We have calculated that if all dendrites entered with a diameter of 0.3  $\mu\text{m}$  were actually 0.1  $\mu\text{m}$  in diameter (an unlikely occurrence), the volume estimate would be decreased by approximately 20%. Thus, the true volume of neurons in CA3 may lie somewhere between the estimates provided above and numbers 20% smaller than these estimates. Average surface area estimates for CA3 and CA2 neurons were also generated; again, they did not include the surface of

dendritic spines. They were: proximal CA3, 12,074  $\mu\text{m}^2$ ; mid CA3, 16,932  $\mu\text{m}^2$ ; distal CA3, 19,255  $\mu\text{m}^2$ ; very distal CA3, 23,499  $\mu\text{m}^2$ ; and CA2 24,619  $\mu\text{m}^2$ . This parameter was somewhat more susceptible to differences in the diameter and these numbers would be decreased by as much as 35% if dendrites entered into the computer with a diameter of 0.3  $\mu\text{m}$  actually had a diameter of 0.1  $\mu\text{m}$ .

#### Dendritic organization of CA2 pyramidal cells

The overall organization of the dendritic trees of CA2 pyramidal cells was similar to that of the CA3 neurons

### CA3 Neuron (C31164)



### CA1 Neuron (C9236E)

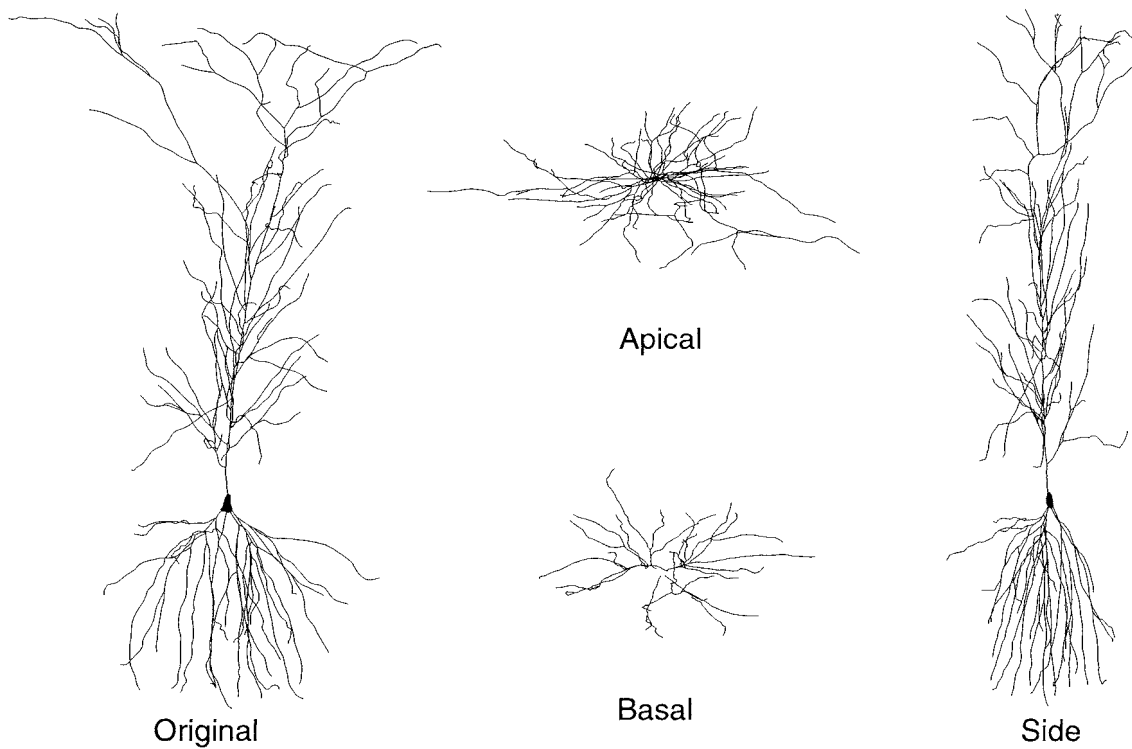


Fig. 6. Four computer generated views of a CA3 pyramidal cell (**Top**) and a CA1 pyramidal cell (**Bottom**). The plots show the neuron in its original position (original) and viewed from the side (side) i.e. showing the septotemporal extent of the neuron. The basal dendrites

(basal) are shown as if viewed from the bottom of the neuron and the apical dendrites (apical) are shown as if viewed from the top. Note that the apical dendrites of the CA1 cell are asymmetric; they tend to be somewhat longer in the transverse axis than in the septotemporal axis.

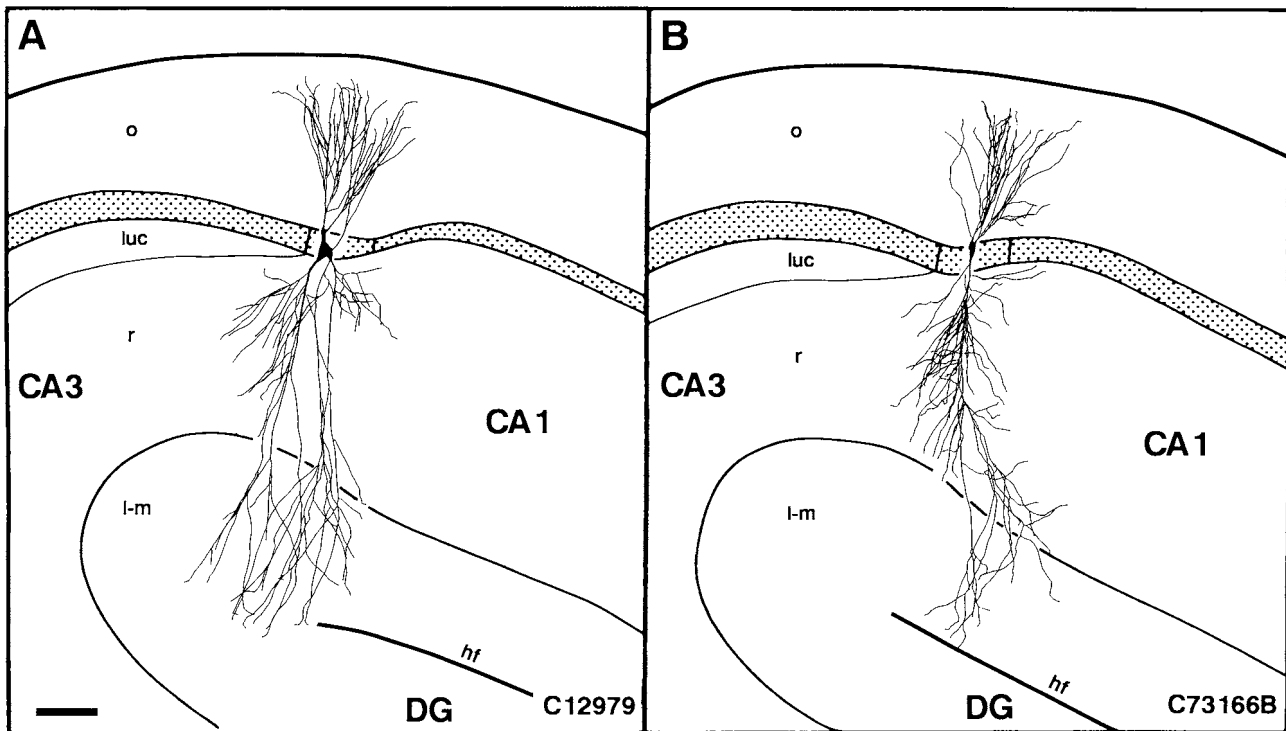


Fig. 7. Computer generated line drawings of a CA2 neuron (**A**) and a "CA1" cell (**B**) located within the cytoarchitectonically defined CA2 region. The latter neuron is considered to be a CA1 pyramidal cell because of its similarities with neurons located within the CA1 field. Comparison of these two neurons emphasizes the distinctiveness of CA2 and CA1 neurons. The CA2 neuron (**A**) has a larger cell body and the dendrites in stratum radiatum demonstrate side branches only in

the deep four fifths of the layer. The CA1 neuron (**B**) has a smaller cell body and its primary apical dendrite generates side branches throughout stratum radiatum. Interestingly the distal apical dendrites of the CA2 pyramidal cell do not enter stratum lacunosum-moleculare of CA1 and the distal dendrites of the CA1 neuron appear to bend substantially to avoid entering stratum lacunosum-moleculare of CA2. Scale bar: 100  $\mu$ m.

located in the distal and very distal portion of the field. The major distinguishing characteristic was the lack of thorny excrescences on the proximal apical dendrites (Figs. 4 and 13). We should emphasize that the much disputed existence of CA2 rests on the notion that there are neurons in this region that have somal sizes similar to cells in CA3 but which do not receive mossy fiber input (at least as indicated by a lack of thorny excrescences on their proximal dendrites). Our data are entirely consistent with the validity of distinguishing a separate CA2 region.

There were some subtle differences in the organization of the CA2 dendrites relative to those observed on distal CA3 cells. In stratum oriens, there was less total dendritic length in the population of CA2 cells than in the distal and very distal CA3 cells. Even though the total dendritic length of the CA2 cells was only slightly less than the very distal CA3 cells, the proportion of the CA2 dendritic tree in stratum oriens (38%) was appreciably less than in any portion of CA3 (Table 1). In stratum radiatum, the dendritic pattern closely matched that of the CA3 cells, i.e. the plexus of side branches only occurred in the deep four fifths of the layer and there were few side branches in the superficial "projection zone." (Figs. 4, 7A and 8). The length of dendrites in stratum radiatum of CA2 was slightly higher than in the distal CA3 cells and accounted for approximately 31% of the total dendritic length. The amount of dendritic tree in stratum lacunosum-moleculare of CA2 pyramidal cells was slightly higher than in distal CA3 cells and accounted for approximately 30% of the total dendritic

tree. It should be noted that CA2 dendrites located in stratum lacunosum-moleculare did not extend into CA1 (Fig. 7A). The dendrites in stratum lacunosum-moleculare had the same vertically oriented and transversely constrained appearance that was typical of CA3 cells. The width, depth and height of the CA2 pyramidal cell dendritic trees were similar to those for the CA3 pyramidal cells (Table 1).

As noted previously, the CA2 region appeared to contain a heterogeneous population of pyramidal neurons. Some of the cells that were labeled in this field (C91665, C73166A, C73166B—Table 2) had all of the dendritic characteristics of typical CA1 pyramidal cells and they have been included among the larger population of CA1 cells (Table 2). We consider that these cells, which were found deep in the pyramidal cell layer, were located in the most proximal portion of the CA1 pyramidal cell layer which was overlapped by or intermixed with elements of the distal CA2 region.

### Organization of the CA1 pyramidal cell dendritic trees

At the transition from CA2 to CA1, there is a dramatic change in the organization of pyramidal cell structure (Fig. 15). As noted previously, the cell bodies of pyramidal neurons in CA1 are markedly smaller than those in CA3 and CA2 (Tables 1 and 2; Figs. 10 and 13). Moreover, the configuration of the dendritic trees of these cells had a

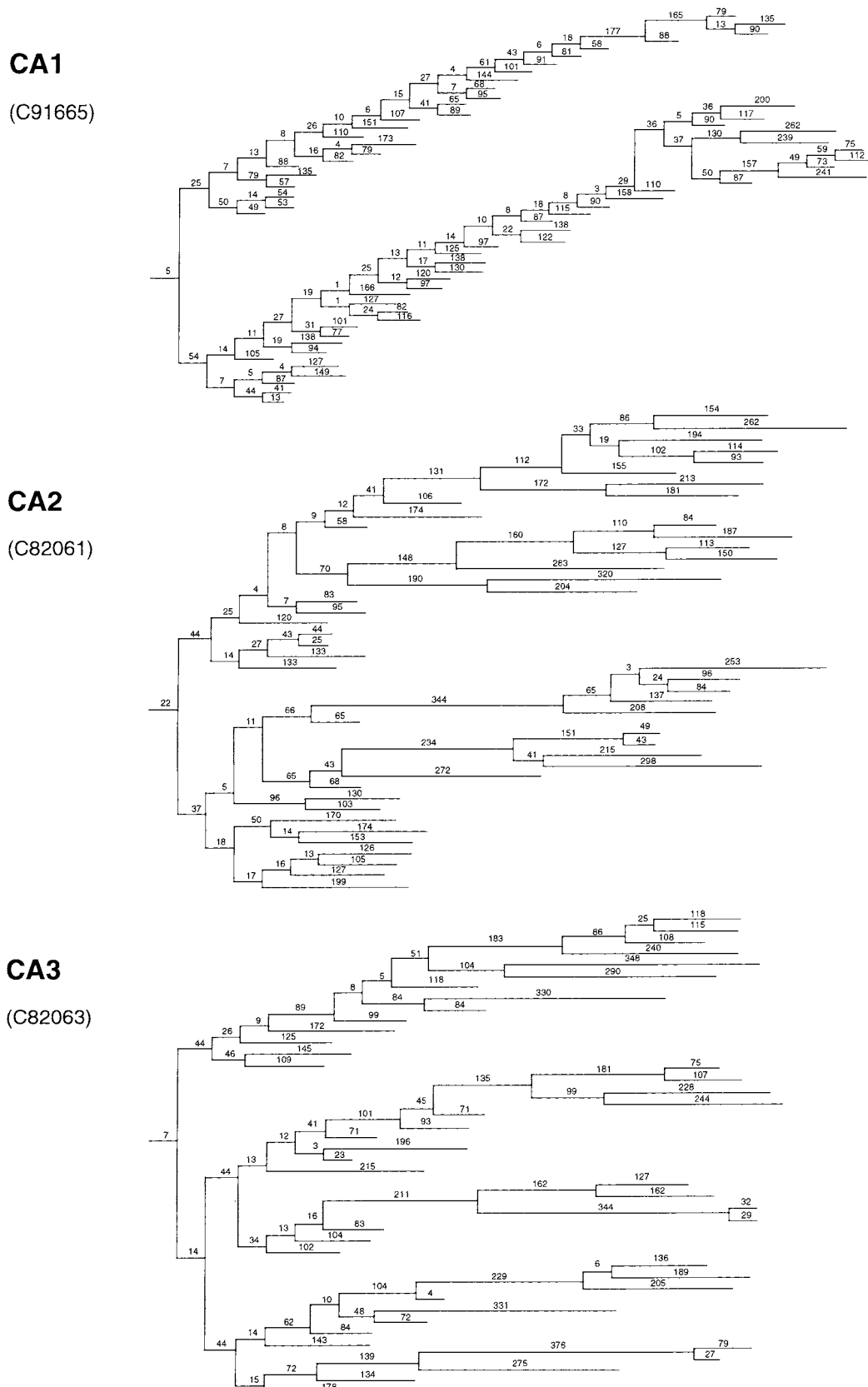


Fig. 8. Computer generated dendritic tree diagrams illustrating the number and lengths of segments of the apical dendrites for a CA1, CA2 and CA3 pyramidal cell. Note that the side branches of CA1 cells are given off throughout stratum radiatum whereas those in CA3 and CA2 are given off only from the proximal portions of secondary dendrites.

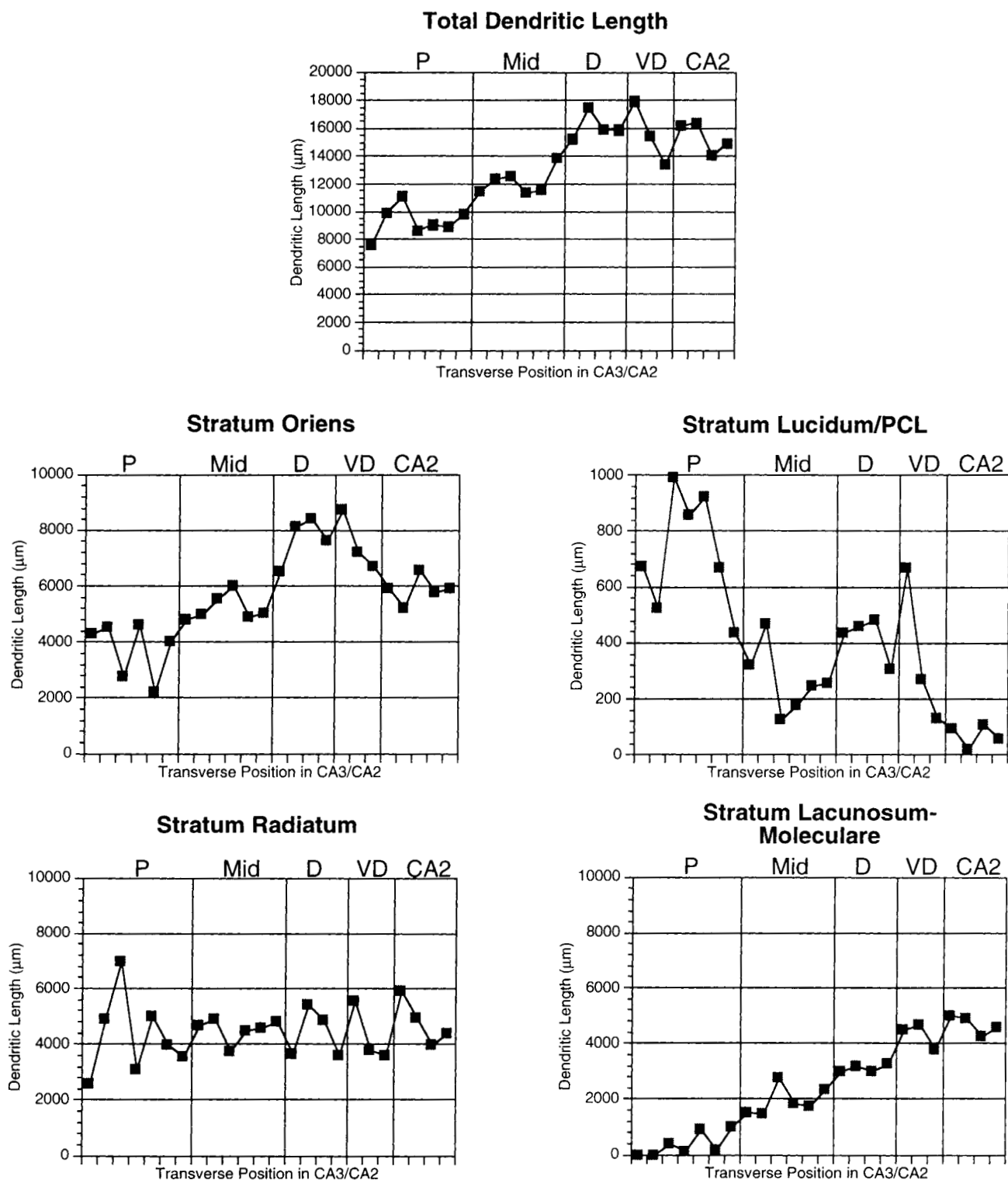


Fig. 9. Graphs illustrating the laminar distribution of dendrites for CA3 neurons located at different positions within the field and for CA2 neurons. The summed dendritic segments in each of the laminae of the hippocampus are plotted for groups of cells located in the proximal (P) and middle (Mid) distal (D) and very distal (VD) portions of CA3 and within

CA2. Note that total dendritic length increases along a proximodistal gradient. An equally clear gradient of increasing dendrite length occurs in the stratum lacunosum-moleculare. The length of dendrites in stratum radiatum, in contrast, is relatively stable throughout CA3 and CA2. See text for further details.

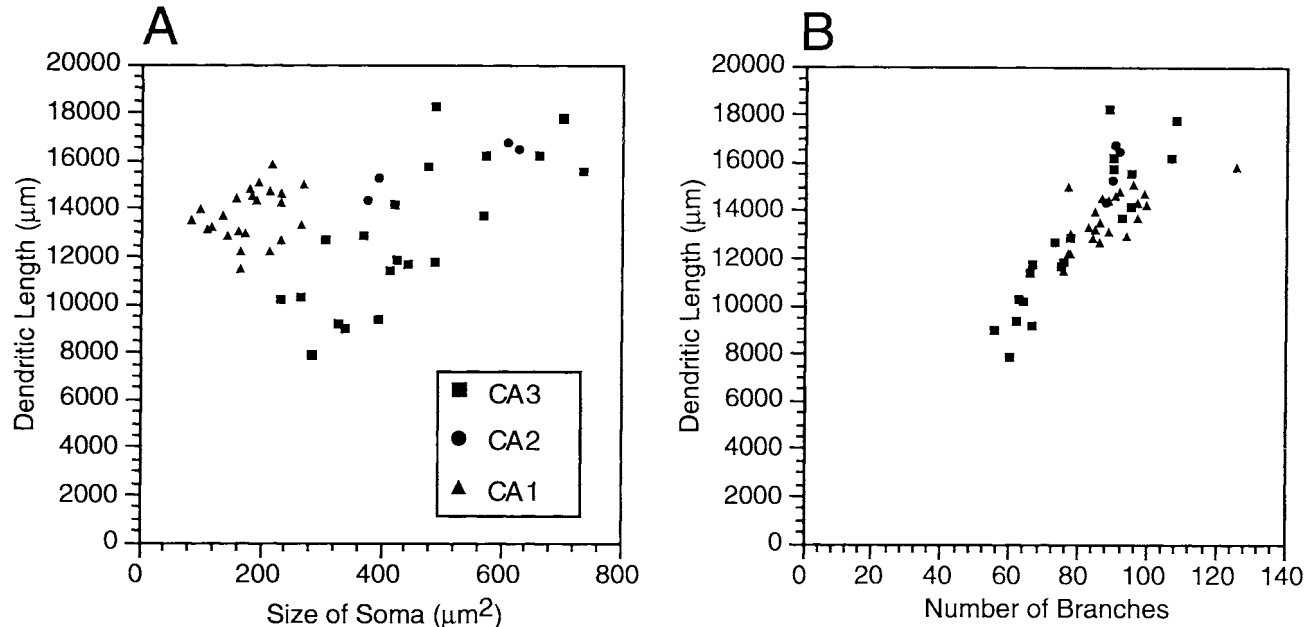


Fig. 10. **A.** Scatter plot illustrating the relationship between cross sectional area of pyramidal cell somata and the total length of the dendritic tree. CA1 cells tend to have smaller and more homogeneous cell somata. The size of CA3/CA2 cell somata appear to be linearly related to the overall length of the dendritic tree. **B.** Scatter plot

illustrating the relationship between the number of dendritic branches and the total dendritic length. The total length of the dendritic tree appears to increase in relation to the number of dendritic branches the neuron generates.

distinctly "CA1" appearance. This is perhaps best appreciated in Figure 7, which illustrates a CA2 cell (Fig. 7A) and a CA1 cell (Fig. 7B) that is located close to the CA2/CA1 border. The CA1 cell, for instance, has dendritic side branches throughout stratum radiatum; the CA2 pyramidal cell, in contrast, does not have branches in the projection zone. Interestingly, the distal apical dendrites of the CA1 cell avoided entering the stratum lacunosum-moleculare of the CA3/CA2 field and bent distally to enter this layer above a region that was clearly within CA1.

The most striking finding concerning the dendritic organization of CA1 cells was that, as a population, they were far more homogeneous than the CA3/CA2 cells (Fig. 15). This is readily apparent from Table 2, which indicates that the mean total dendritic length of CA1 cells was 13,424  $\mu\text{m}$  with a standard deviation of only 1,034  $\mu\text{m}$ . The homogeneity of the CA1 cells can also be appreciated in Figure 12, in which 6 pyramidal cells from the mid region of CA1 are illustrated. While there were some subtle differences in the number or orientation of dendritic branches, the general form of the dendritic tree was remarkably similar from neuron to neuron.

In general, CA1 pyramidal cells demonstrated 1 or 2 primary apical dendrites (Table 2; Figs. 11 and 12). In some cases, both apical dendrites arose directly from the neuronal cell body. This characteristic appeared to be somewhat more common for neurons located either deep in, or slightly below, the pyramidal cell layer (Figure 12—CD0351). In other neurons, a single primary apical dendrite emerged from the neuronal cell body and then divided either within stratum radiatum or, on occasion, only after entering stratum lacunosum-moleculare. Between 1 and 5 primary basal dendrites originated from CA1 cell bodies and these typically bifurcated two or three times before terminating near the alveus.

The dendrites of stratum oriens had a mean length of 4,586  $\mu\text{m}$  which accounted for approximately 34% of the total dendritic tree (Table 2). This was a lower percentage of the total dendritic tree than was observed for CA3/CA2 cells (38–51%). The converse was true in stratum radiatum, however. In this layer, the mean dendritic length for CA1 cells was 6,307  $\mu\text{m}$  which accounted for approximately 47% of the total dendritic length. This can be contrasted with a mean dendritic length of 4,452  $\mu\text{m}$  for CA3/CA2 cells. The percentage of dendritic tree in stratum radiatum of CA1 was roughly similar to the percentage on pyramidal cells located in the proximal portion of CA3 which had about 46% of their dendritic tree in stratum radiatum. The latter, however, had little or none of their dendritic tree in stratum lacunosum-moleculare. For the more typical CA3 cells in the mid to distal CA3, the percentage of dendrite in stratum radiatum ranged from 27–37%. The increased length of the dendritic tree in stratum radiatum of CA1 is undoubtedly accounted for by the occurrence of side branching throughout the full radial extent of the layer. The mean number of apical terminal dendritic branches in CA1 (62) is substantially higher than the number in CA3 (40) and in CA2 (52) (Tables 1 and 2; Figure 8) and most of these occur as side branches in stratum radiatum. Interestingly, an analysis of the lengths of side branches in stratum radiatum of CA1 and CA3 indicated that they were of approximately equal lengths in both regions. The lengths of a sample of 16 CA3 cells (with 429 side branches measured) and 7 CA1 cells (with 411 side branches measured) indicated that the mean length of stratum radiatum side branches on CA3 cells was  $100.5 \pm 40.0 \mu\text{m}$  while the mean length of side branches in CA1 was  $114.9 \pm 42.2 \mu\text{m}$ . Thus, the increased length of dendrites in stratum radiatum of CA1 relative to CA3 can only partially be accounted for by an increased length of individual side branches.

HIPPOCAMPAL PYRAMIDAL CELL DENDRITES

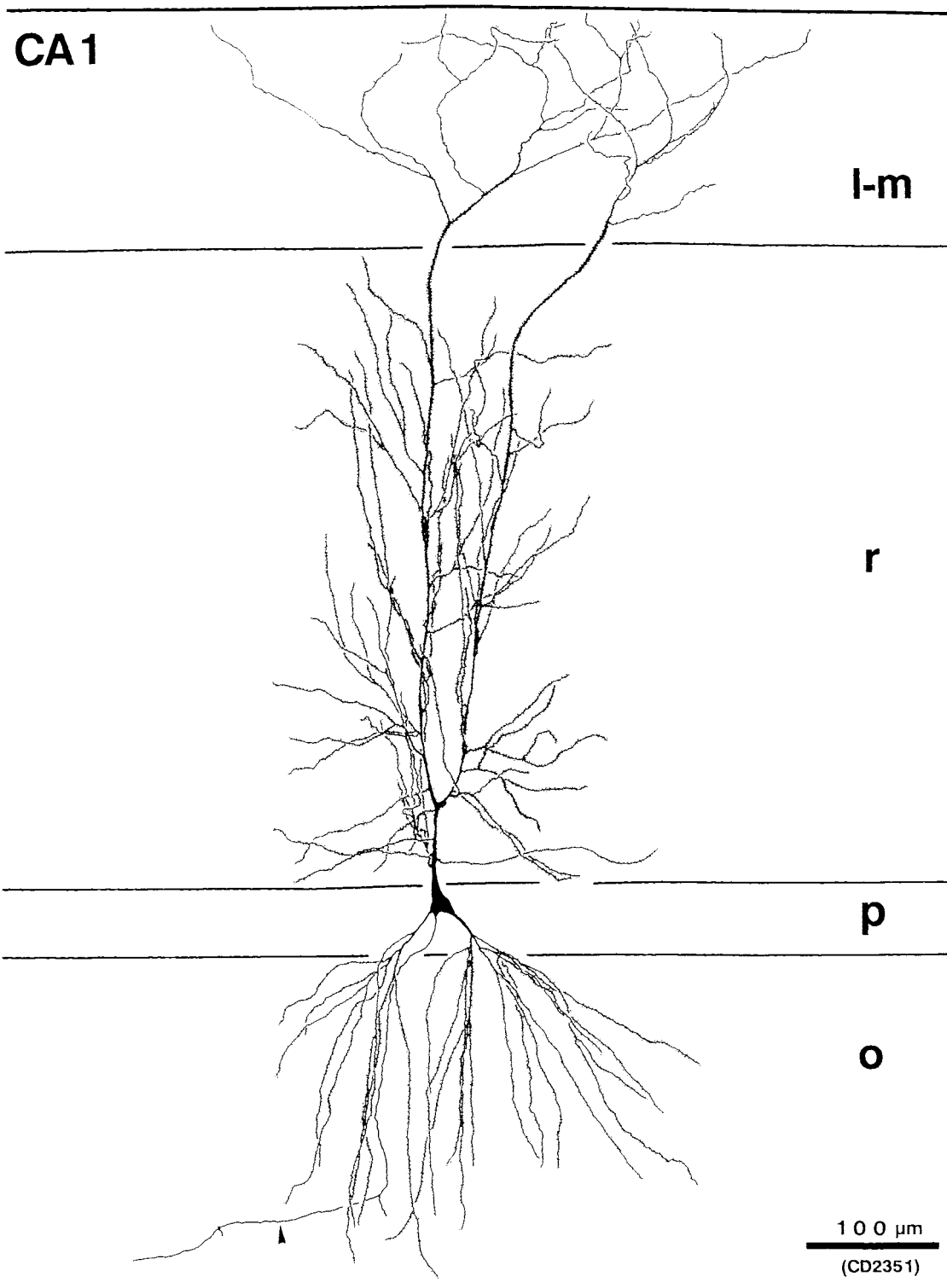


Fig. 11. Camera lucida line drawing of a CA1 pyramidal cell from the mid portion of the field. Note that side branches originate from the primary dendrites throughout the full extent of stratum radiatum. Note also the curved and irregular trajectories of dendritic branches in the stratum lacunosum-moleculare. The axon of this cell is indicated with an arrowhead.

The CA1 distal dendritic branches located in stratum lacunosum-moleculare were substantially different from

of dendrite in this region was about 2,532  $\mu\text{m}$  which accounted for approximately 19% of the total dendritic tre

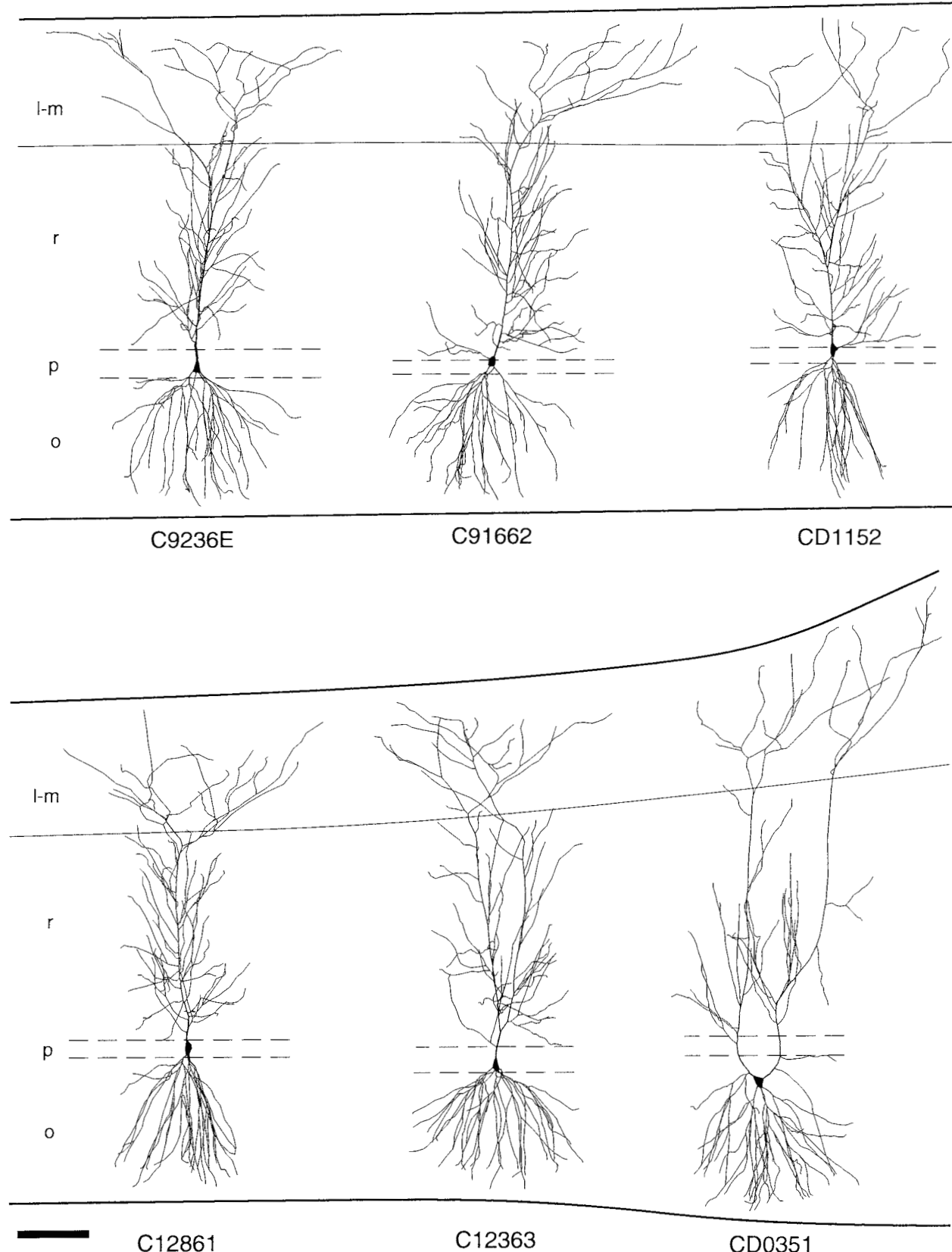


Fig. 12. Computer generated line drawings of CA1 pyramidal cells from the mid two thirds of the field. Proximal CA1 (towards CA2) is to the left of the upper row and distal CA1 (towards the subiculum) is to the right of the lower row. CA1 pyramidal cells typically demonstrate either 1 primary apical dendrite, as in C9236E, or 2 primary apical dendrites, as in CD0351. Scale bar: 100  $\mu$ m.

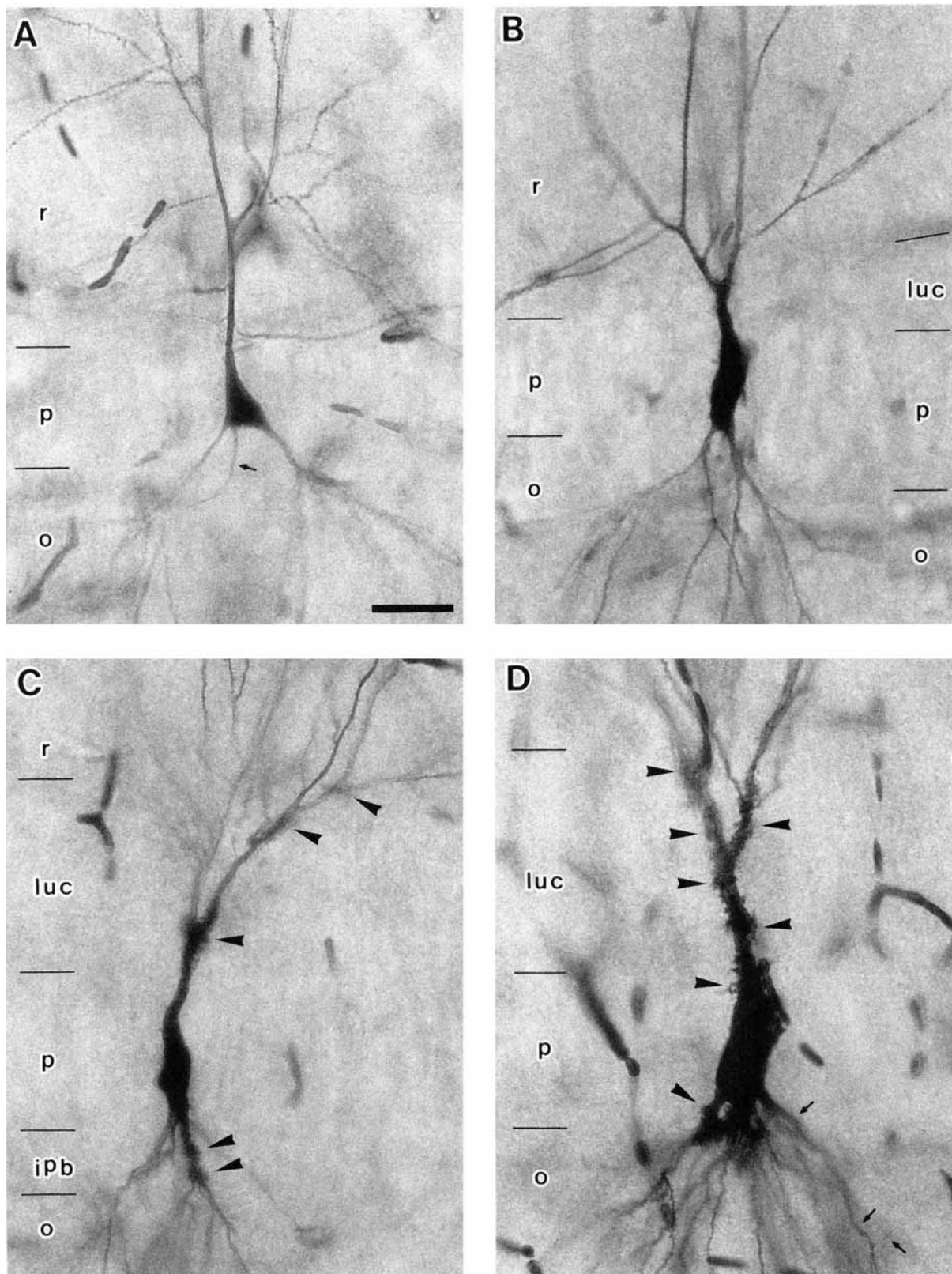


Fig. 13. Photomicrographs of intracellularly labeled pyramidal cells in CA1 (**A**), CA2 (**B**) and CA3 (**C and D**). Small arrows indicate the initial portion of the axon and axonal collaterals. Arrowheads indicate thorny excrescences. **A.** CA1 cell seen in Figure 11 (CD2351). A number of dendritic side branches are given off from the primary and secondary dendrites in the stratum radiatum. The side branches and the secondary dendrites demonstrate many typical spines, but no spines are observed on the surface of the primary dendrite. **B.** CA2 cell seen in Figure 4 (C12971). The left side of the picture is the CA1 sector and the right side is the CA3 sector. No thorny excrescences are seen on the

apical and the basal dendrites. **C and D.** Proximal (C60463) and distal (C10861) CA3 cells respectively. Thorny excrescences tend to form large clusters on the proximal portion of the apical and basal dendrites. Note that the distal CA3 cell (**D**) has thorny excrescences which cover virtually all of the surface of the primary dendrite and the proximal portion of the secondary apical dendrites in stratum lucidum. Note also that a large cluster of the thorny excrescences is also located on the proximal portion of the basal dendrite. Scale bar in **A** equals 30  $\mu$ m and applies to all panels.

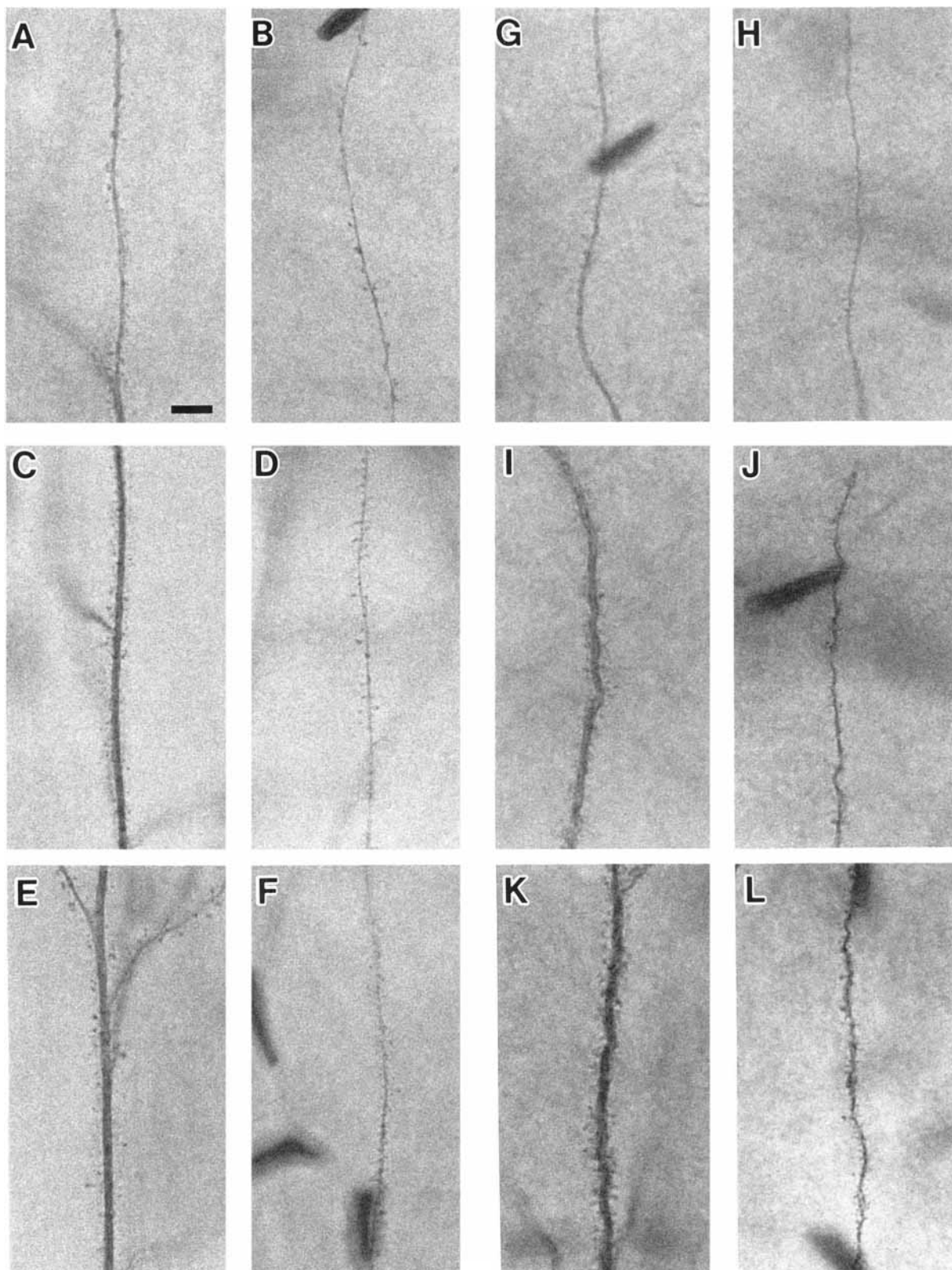


Fig. 14. Photomicrographs of spiny dendritic segments from pyramidal cells in CA1 (A–F, CD2351) and CA3 (G–L, C10861) from different laminae. Thick (A) and thin (B) branches of CA1 dendrites in the stratum lacunosum-moleculare. Proximal (E) and distal (C) portion of the secondary dendrite and a side branch (D) of a CA1 cell; these processes are located in stratum radiatum. A basal dendrite of CA1 cell

located in stratum oriens (F). A secondary dendrite (G) and a fine branch (H) of a CA3 cell located in stratum lacunosum-moleculare. Secondary dendrites of CA3 cell in the proximal portion of the stratum radiatum (K) and in the projection zone (I). A side branch (J) in the stratum radiatum. A branch of the basal dendrite (L) in the stratum oriens. Scale bar in A represents 5  $\mu\text{m}$  and applies to all panels.

(4–30%). The orientation of the CA1 dendrites in stratum lacunosum-moleculare, however, was different from that in CA3/CA2. As illustrated in Figures 6, 11 and 12, upon entering stratum lacunosum-moleculare, the CA1 pyramidal cell dendrites tended to travel transversely and extended somewhat beyond the width occupied by dendrites in stratum radiatum or stratum oriens (Fig. 6). Dendrites in this layer tended to have a much less linear appearance and extended towards the hippocampal fissure in a curved fashion. As illustrated in Figure 11, the density of spines decreased substantially on the dendrites located in stratum lacunosum-moleculare (see also Fig. 14).

Despite the more oblique orientation of dendrites in the stratum lacunosum-moleculare, the mean maximal width of the CA1 dendritic trees was approximately 430  $\mu\text{m}$  or about the same as the width of the CA3 and CA2 dendritic trees (see also Fig. 15). The mean septotemporal extent of the CA1 neurons was approximately 300  $\mu\text{m}$  or again just about the same as CA3 and CA2 cells. The average height of the CA1 pyramidal cells was approximately 920  $\mu\text{m}$  and, unlike the CA3 cells, the height was nearly uniform in all of the labeled CA1 pyramidal cells.

As noted previously, some of the CA1 pyramidal cells contained 1 primary apical dendrite while others contained 2 or 3. Given the relative homogeneity of the CA1 population, we evaluated whether parameters of the dendritic tree varied in a consistent fashion depending on the number of apical primary dendrites. As indicated in Table 3, the number of neurons in our population with 2 ( $n = 6$ ) or 3 ( $n = 2$ ) primary dendrites was small but some interesting trends appeared to emerge in our analysis. Thus, CA1 pyramidal cells with 1 primary dendrite tended to have fewer terminal apical dendritic branches ( $57.4 \pm 6.6$ ) than neurons with 2 ( $63.8 \pm 9.4$ ) or 3 (87) apical dendrites. Similarly, the apical dendritic tree tended to be shorter in cells with only 1 apical dendrite ( $8,300 \mu\text{m} \pm 745$ ) than in cells with 2 ( $9,441 \mu\text{m} \pm 958$ ) or 3 ( $11,062 \mu\text{m} \pm 447$ ) primary apical dendrites. The total dendritic length of CA1 cells followed the same progression. Interestingly, there was a slight tendency for CA1 pyramidal cells with only 1 apical dendrite to have a greater number of terminal basal dendrites ( $30.7 \pm 5.5$ ) than cells with 2 ( $27.2 \pm 3.5$ ) or 3 ( $27.5 \pm 9.1$ ) apical dendrites. And the greater number of basal dendritic branches meant that CA1 pyramidal cells with a single apical dendrite tended to have a somewhat larger basal dendritic tree ( $4,845 \mu\text{m} \pm 837$ ) than neurons with 2 ( $4,338 \mu\text{m} \pm 374$ ) or 3 ( $3,389 \mu\text{m} \pm 1805$ ) apical dendrites. These data appear to indicate that the homogeneity of total dendritic length in the population of CA1 pyramidal cells is produced, in part, by maintaining a balance between the amount of dendritic tree that is accounted for by the basal and apical dendrites i.e., a smaller apical dendritic plexus is compensated for, in part, by a larger basal dendritic plexus.

As with the CA3/CA2 neurons, we were able to generate an estimate of the total neuronal volume and surface areas from the three dimensional digitizing program. The mean neuronal volume for the entire population of CA1 pyramidal cells was  $1,940 \mu\text{m}^3$  and the mean neuronal surface area was  $15,006 \mu\text{m}^2$ . Interestingly, the volume estimates did not vary much for neurons with 1, 2 or 3 primary dendrites (1 primary dendrite  $1,941 \mu\text{m}^3$ ; 2 primary dendrites  $1,947 \mu\text{m}^3$ ; 3 primary dendrites,  $1,908 \mu\text{m}^3$ ). As discussed above, if the finest dendritic branches had been  $0.1 \mu\text{m}$  rather than  $0.3 \mu\text{m}$  (which was entered into the computer), the mean volume estimate for one of the labeled CA1 cells (C91665)

would have decreased to  $1,727 \mu\text{m}^3$  from  $2,388 \mu\text{m}^3$  or a 28% decrease. Thus, it is likely that the true volume of neurons lies somewhere between the estimated volume and a figure 28% smaller.

## DISCUSSION

The current study provides the first comprehensive, quantitative analysis of the dendritic trees of rat hippocampal pyramidal cells. Neurons in the CA1, CA2 and CA3 regions of the hippocampus were intracellularly injected with HRP in the *in vitro* slice preparation using 400  $\mu\text{m}$  thick slices from mature, female rats. The entire 400  $\mu\text{m}$  slices were processed histologically without further sectioning for visualization of the tracer filled neuron which was subsequently subjected to computer-aided digitization. These procedures produced estimates of total dendritic length that far exceeded numbers published in the literature from previous Golgi studies. Moreover, the reliability of the labeling and analysis procedures demonstrated distinct differences in the structure of CA3 dendritic trees that depended on the proximodistal location of the cell body. We were also able to demonstrate a remarkable homogeneity of dendritic structure of neurons distributed throughout the CA1 region.

### Cells labeled in the *in vitro* slice preparation have longer dendritic trees than those labeled in Golgi preparations

Despite the substantial literature on the neuroanatomical analysis of the rat hippocampal formation, there is remarkably little quantitative data on the dendritic organization of hippocampal pyramidal cells. And many of these data are based on the analysis of Golgi preparations. Moreover, many of these data have been derived from analysis techniques (such as the Sholl analysis) which we have not carried out on our population of labeled neurons and thus direct comparison is not possible. However, in those cases in which similar dendritic length measurements have been made, the neurons described from the Golgi preparations are invariably reported to have smaller dendritic trees than we have observed. Pokorny and Yamamoto (1981), for example, used the Golgi-Cox technique to evaluate the development of dendrites in the CA1 region of the rat. The group of their animals that most closely matched ours were 48 days old when sacrificed. They reported that the mean total dendritic length of their population of CA1 neurons was  $4,432 \mu\text{m}$  whereas our mean total dendritic length was  $13,424 \mu\text{m}$ . It is difficult to know to what extent this marked difference is attributable to shrinkage of the tissue in their preparations or to the fact that many of the dendrites that they measured had been amputated in the sectioning process (see below). They found that 41% of the dendritic tree was located in stratum oriens, 48% in stratum radiatum and 11% in stratum lacunosum-moleculare. While the percentage of dendritic tree in stratum radiatum was similar in our population, we had a lower percentage (34%) of the dendritic tree in stratum oriens but a much higher percentage (19%) in stratum lacunosum-moleculare. Thus, part of the smaller size of the dendritic trees of their CA1 pyramidal cells could be accounted for by the paucity of distal apical dendrites on their sampled neurons. It is likely that many of the distal tips of the dendrites on their neurons were transected since they employed histological sections that were only  $150 \mu\text{m}$  thick. We found that the

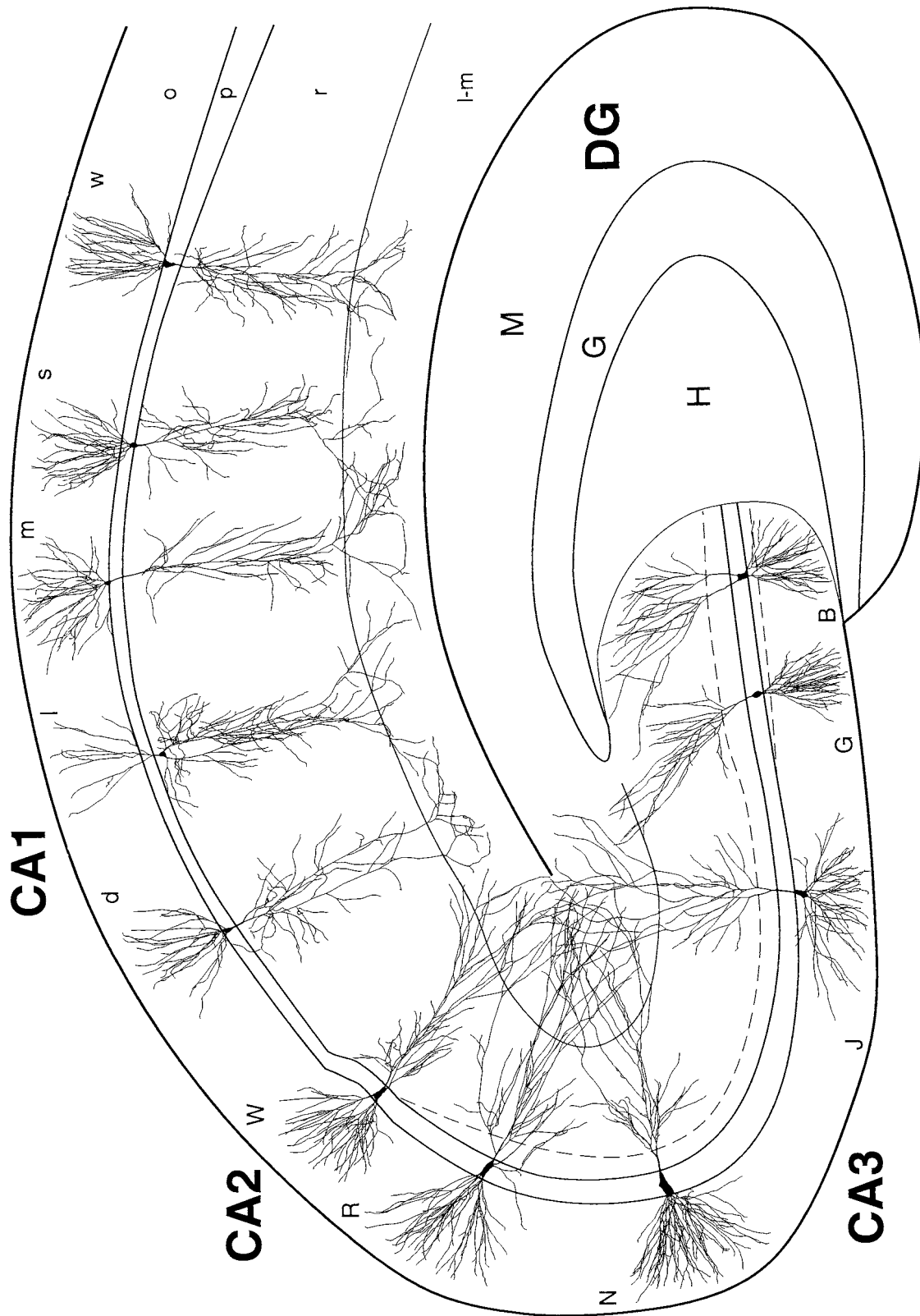


Fig. 15. Summary illustration of the organization of hippocampal pyramidal cells. Produced as a composite of computer generated line drawings of neurons from CA3, CA2 and CA1. Letters adjacent to neurons provide index to cell data in Tables 1 and 2. Dashed line in CA3 marks region of infra- and suprapyramidal mossy fibers. Abbreviations marking layers of the hippocampus are indicated at top right.

Fig. 15. Summary illustration of the organization of hippocampal pyramidal cells. Produced as a composite of computer generated line drawings of neurons from CA3, CA2 and CA1. Letters adjacent to neurons provide index to cell data in Tables 1 and 2. Dashed line in CA3 marks region of infra- and suprapyramidal mossy fibers. Abbreviations marking layers of the hippocampus are indicated at top right.

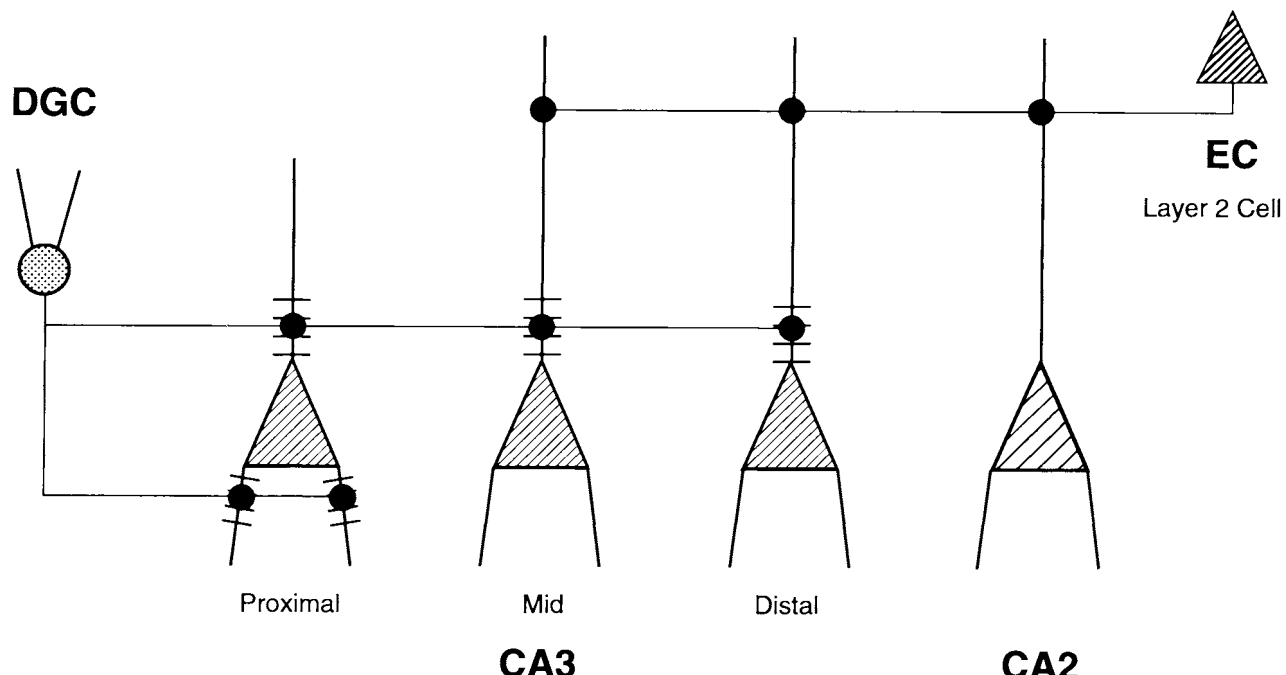


Fig. 16. Schematic diagram representing the termination of the perforant path and the mossy fiber projection within different portions of CA3. Pyramidal cells located proximally in CA3 receive mossy fiber innervation on both apical and basal dendrites. These same neurons do not have dendrites located in stratum lacunosum-moleculare, however, and thus receive little or no perforant path input. At the opposite extreme of the distribution, CA2 pyramidal cells receive no mossy fiber input but have a substantial portion of their dendritic trees in stratum

lacunosum-moleculare. Since the perforant path projection to the dentate gyrus and CA3/CA2 regions arises as collaterals from the same layer II entorhinal neurons, it is likely that neurons within CA3/CA2 will be differentially influenced by monosynaptic versus disynaptic activation from the entorhinal cortex. Short line segments on the proximal dendrites of the CA3 neurons indicate positions of mossy fiber thorny excrescences.

thickness (i.e. the septotemporal extent) of the CA1 dendritic tree was at least 260  $\mu\text{m}$ . The fact that Pokorny and Yamamoto (1981) found that the mean length of dendritic side branches in stratum radiatum was only approximately 54  $\mu\text{m}$ , whereas these branches in our population were approximately 100  $\mu\text{m}$ , further supports the suggestion that many of the distal portions of the dendrites throughout the dendritic tree were severed in the sectioning process. In a similar study, Haschke et al. (1980) used rapid Golgi methods to study the development of CA1 pyramidal cells; their oldest population of rats was 20 days old. In this population of CA1 neurons, the mean total dendritic length was 5,401  $\mu\text{m}$ . While the total dendritic length in this study was approximately half the number found for our CA1 cells, the percentages of dendritic tree in the various laminae were very similar to those that we found. Perhaps, the younger age of this population of neurons accounts, at least in part, for the smaller size of the dendritic trees.

Beyond the problems of complete staining and of visualizing the bulk of the dendritic trees in relatively thin histological sections, there is an additional purely technical reason why dendritic trees in Golgi preparations may be substantially smaller than those in our preparations. As noted in the Methods section, the hippocampal slices used in the present study were cleared with ascending concentrations of glycerol and ultimately stored in 100% glycerol. This provided excellent transparency of the slice with little or no shrinkage of the tissue (see Claiborne et al., 1986). In standard Golgi processing, tissue is subjected to complete

alcoholic dehydration either before coverslipping or prior to being embedded in nitrocellulose for sectioning. This procedure leads to substantial shrinkage of the tissue. Grace and Llinás (1985) formally evaluated the amount of shrinkage of a 300  $\mu\text{m}$  thick slice that was subjected to standard histological processing. They found that the slice decreased to an average of 67% in linear dimension and decreased to 46% in area. While not quantitatively analyzed, they also demonstrated that intracellularly labeled neurons shrank substantially in height during the dehydration process. Thus, part of the explanation for the smaller cells in the Golgi preparations is that the tissue typically shrinks appreciably during processing. While correction factors could be employed to compensate for this shrinkage, it is equally clear that labeling neurons within a thick hippocampal slice and analyzing the slice without further sectioning is perhaps more significant in achieving accurate reconstruction and measurement of the entire hippocampal pyramidal cell dendritic trees.

#### Comparison with results from previous intracellular staining studies

Turner and Schwartzkroin (1983) analyzed a variety of dendritic parameters from guinea pig hippocampal pyramidal cells that were intracellularly injected with horseradish peroxidase; length measurements were made from two dimensional camera lucida drawings. Their sample of 11 CA3 cells had a mean total dendritic length of 11.5 mm

whereas their population of 6 CA1 neurons had a mean total dendritic length of 8.4 mm. The transverse location of these neurons within the pyramidal cell layer was not indicated. More recently, Trommald et al., (1995) have evaluated the dendritic lengths of a population of 7 rat CA1 pyramidal cells that were injected with Lucifer Yellow in the *in vitro* slice preparation using the confocal laser microscope. These authors focused on the organization of the basal dendritic tree and found that the mean total dendritic length for basal dendrites was approximately 4,500  $\mu\text{m}$ . This is in good agreement with the mean estimate of 4,585  $\mu\text{m}$  of dendrite in stratum oriens for our population of CA1 pyramidal cells. Trommald's et al. (1995) estimate of total dendritic length (11,900  $\mu\text{m}$ ) is somewhat lower than our mean of 13,424  $\mu\text{m}$ . What is most consistent, however, is the finding that these intracellular injection techniques, regardless of the analytic method, provide estimates of total dendritic length that are much larger than estimates from previous Golgi studies.

### **Pyramidal cells in the CA3 region demonstrate substantial variability in their dendritic trees depending on their proximodistal positions**

As illustrated in Figure 15, the dendritic trees of pyramidal cells in the CA3 region showed substantial variation in their shape and size. In general, cells closest to the dentate gyrus had the shortest dendritic trees while those in the distal portion of the field had the longest dendrites. While the number of cells labeled in the most proximal portion of CA3 was not large, we found that their dendrites typically did not enter the hilus of the dentate gyrus. Moreover, cells in this region either did not have any dendrites which entered the stratum lacunosum-moleculare or had only a few elongated apical dendrites that bent around the tip of the suprapyramidal limb of the dentate gyrus to enter stratum lacunosum-moleculare. At progressively more distal positions within CA3, cells had progressively more of their dendritic tree within stratum lacunosum-moleculare. While the amount of dendrite in stratum radiatum tended to be rather constant throughout the transverse extent of CA3, there was an increase in the amount of dendrite located in stratum oriens at progressively more distal portions of the field. Finally, the amount of dendrite contained within the domain of the mossy fibers was highest for the proximal CA3 cells (where there was both a suprapyramidal and infrapyramidal bundle of mossy fibers) and smallest in the distal portion of the field. The CA2 pyramidal cells were at the extreme end of this distribution since they did not receive any mossy fiber input.

Perhaps the most clear cut implication of the variation in size and distribution of CA3 pyramidal cell dendritic trees is that cells in different transverse portions of the field will be innervated by different proportions of two of their major inputs, i.e., the mossy fibers and the perforant path. As schematized in Figure 16, cells in the proximal portion of CA3 receive little or no perforant path input since their dendrites do not extend into stratum lacunosum-moleculare. However, since both the apical and basal dendrites of these cells are innervated by mossy fibers, it is likely that they receive a more substantial mossy fiber input. Since there are no data available on the exact number of mossy fiber terminations on CA3 cells in different portions of the field, this speculation awaits experimental verification. However, it would be interesting if there was a gradual decline in mossy fiber termination at progressively more

distal portions of CA3 with the culmination of the gradient occurring in CA2, where neurons receive no mossy fiber input (Fig. 13). Claiborne (personal communication) has made observations that are consistent with this hypothesis. She and her colleagues counted "clusters" of thorny excrescences on the proximal dendrites of CA3 pyramidal cells in different transverse portions of the field. Clusters were counted because it was difficult or impossible, in many cases, to identify individual thorns at the light microscopic level. Claiborne found that proximal CA3 neurons demonstrated approximately 12 clusters of thorns on their apical dendrites and 10 on their basal dendrites. Cells in the distal portion of the field had approximately 13 clusters of thorns on their apical dendrites but only 1 cluster on their basal dendrites (many neurons had no clusters at all on their basal dendrites). These observations suggest that proximal neurons may have nearly twice as much mossy fiber input as cells located more distally.

In contrast to the mossy fiber input, cells located at distal portions of CA3 receive a substantial perforant path input. While the amount of dendritic length in stratum lacunosum-moleculare cannot be used as an absolute indicator of perforant path input, the increasing total dendritic length in this layer in neurons at progressively more distal portions of CA3 (Fig. 9), is suggestive that there may be a progressive increase in the amount of perforant path input. Thus, proximally situated CA3 cells will be more exclusively influenced by perforant path information that is first processed through the dentate gyrus, whereas more distally placed cells will receive perforant path inputs both monsynaptically (through direct entorhinal projections) and disynaptically through the dentate gyrus. It is important to point out that the perforant path projections to the dentate gyrus and to the CA3/CA2 fields arise from the same layer II cells in the entorhinal cortex (Steward and Scoville, 1976) and that the two projections are likely to be collaterals of the same neurons (Tamamaki and Nojo, 1993).

The idea that neurons in different transverse portions of the CA3 field might have distinct connections is also consistent with our previous PHA-L analysis of the intrinsic circuitry of CA3 (Ishizuka et al., 1990). We found that the distribution of CA3 connections to CA1 was dependent on the transverse position of the cells of origin. Cells located proximally in CA3 tended to project to distal portions of CA1 and to the more superficial portions of stratum radiatum. CA3 cells located distally, in contrast, tended to project proximally in CA1 and more heavily to stratum oriens than to stratum radiatum (See Ishizuka et al., 1990 for a more detailed description of the topographic organization of CA3 to CA1 projections). We also found differences in the extent and distribution of intrinsic CA3 associational connections. Proximal CA3 cells, for example, gave rise to very limited associational connections within CA3 and these tended to be distributed only to other portions of proximal CA3. CA3 cells located in the middle and distal portions of the field, in contrast, gave rise to massive associational connections that innervated all transverse regions of the field.

Masukawa et al., (1982) analyzed the properties of hippocampal pyramidal cells in mid and distal portions of the CA3 field in the guinea pig *in vitro* slice preparation. They found that depolarization induced bursting activity was more likely for neurons located distally in CA3 than those found in mid CA3. Bilkey and Schwartzkroin (1990) conducted a similar study but found that depolarization

induced spiking was equally likely in pyramidal cells located throughout the transverse extent of CA3. They did find, however, that CA3 pyramidal cells located deeper in the pyramidal cell layer had both a longer, unbranched portion of apical dendrite and a substantially higher probability of generating bursts of spikes. Our population of filled CA3 neurons was too small to detect differences in dendritic parameters based on the location of the cell body within the pyramidal cell layer.

### **CA3 dendrites in stratum radiatum show laminar differences related to the location of associational versus projection fibers**

The distribution of CA3 pyramidal cell apical dendritic side branches within stratum radiatum demonstrated a striking laminar organization. First, in contrast to the observation of Lorente de Nó (1934) who claimed that CA3 pyramidal cells have no side branches, we found that all CA3 pyramidal cells had such branches. And as indicated previously, the total length of the dendritic tree in stratum radiatum was one of the more homogeneous traits of the CA3 pyramidal cell population (Fig. 9). As seen in all of the illustrations of CA3 pyramidal cells (and particularly in Fig. 15), the dendritic side branches in stratum radiatum are found exclusively in the deep four fifths of the layer. In the superficial one fifth of the layer, apical secondary dendrites extend vertically and without branching, until the stratum lacunosum-moleculare is attained. Once within stratum lacunosum-moleculare, dendritic branching begins again.

This pattern of dendritic branching is completely consistent with the laminar distribution of axons in stratum radiatum that we observed in our previous PHA-L study of the CA3 connections (Ishizuka et al., 1990). Cells located in the proximal portion of CA3 give rise to a thick, principal axon which generates a thick collateral (the Schaffer collateral) that ascends into the superficial portion of stratum radiatum and travels transversely into CA1. We observed that most of the axons in this superficial zone of stratum radiatum were thick and lacked varicosities. We proposed that the thick fibers in this region were mainly projection fibers en route to CA1 and generated few synapses en passant within CA3. We therefore dubbed this superficial region of stratum radiatum "the projection zone." The deep four fifths, in contrast, contained numerous varicose fibers of various caliber. It was within this zone, we surmised, that most of the CA3 to CA3 associational and commissural connections were formed. This suggestion has been borne out in a recent electron microscopic analysis of this region (Matsuda and Ishizuka, unpublished observations). The density of synaptic boutons containing spherical vesicles in "the associational zone" of stratum radiatum was found to be approximately 26/100  $\mu\text{m}^2$  whereas in the projection zone this number was only 18/100  $\mu\text{m}^2$ . This result indicates that while contacts appear to be made in higher density in the associational zone (where most of the side branches are located), some contacts are also made in the projection zone. This is consistent with the finding that the secondary dendrites passing through the projection zone do have dendritic spines (Fig. 14I).

### **No distinct types of CA3 pyramidal cells were observed**

We have quantitatively analyzed 20 pyramidal cells at a mid septotemporal level in the CA3 region of the hippocampus. While we can not conclude that this relatively small

population of neurons has sampled all variants of CA3 pyramidal cells in the rat hippocampus, we have not been impressed that the CA3 cells fall into distinct subcategories. Fitch et al., (1989) have proposed, for example, that there are two categories of CA3 pyramidal cells in the rat hippocampus: long-shaft pyramidal neurons and short-shaft pyramidal neurons. We observed CA3 pyramidal neurons with 1–3 primary apical dendrites but they could not easily be dichotomized into long- or short-shafted cells. Thus, the question of whether there are subtypes of CA3 pyramidal cells must await further analysis.

### **CA2 pyramidal cells resemble CA3 pyramidal cells**

Lorente de Nó (1934) first noted that there were a number of differences between neurons in different portions of Ramón y Cajal's (1911) regio inferior. In particular, he observed that some of the large cells at the distal tip of the CA3 field had the same size and dendritic configuration as CA3 pyramidal cells but lacked the distinctive thorny excrescences that were diagnostic of mossy fiber innervation. The identity and uniqueness of the CA2 field has been a matter of ongoing controversy. It now appears, however, that the CA2 field can be distinguished both from CA3 and CA1 by a number of neuroanatomical features (for review see Woodhams et al., 1993).

In the current study, we found that the dendritic trees of CA2 cells greatly resembled those of distal CA3 pyramidal cells. In particular, the proportion of the dendritic tree in each of the major laminae was similar in CA2 and distal CA3 neurons. The branching patterns of the apical dendrites of CA2 and CA3 pyramidal cells were also very similar. Moreover, the distribution of side branches in the deep four fifths of stratum radiatum was similar in CA2 and CA3. The major dendritic characteristic that distinguished CA3 and CA2 pyramidal cells was the lack of thorny excrescences on the latter. We had earlier found that the intrahippocampal projections of the CA2 region had both similarities and differences with the projections arising from the distal CA3 cells (Ishizuka et al., 1990). They were similar in that they projected primarily to CA1 and gave rise to additional associational connections to the CA3 field. These projections were different, however, in that they tended to be much less robust than those that originated from distal CA3 and were distributed in a more diffuse manner within CA1. Taken together with recent evidence that the CA2 region receives certain projections, such as from the supramammillary region (Haglund et al., 1984), that are not directed to CA3, it is clear that CA2 should be considered a distinct subregion of the hippocampus. This conclusion is complicated, however, by the fact that the CA2 region appears to contain a heterogeneous population of pyramidal cells. Some of the neurons that were labeled in this region were much smaller than typical CA2 pyramidal cells and had a dendritic configuration reminiscent of CA1 pyramidal cells. Our interpretation of this finding is that the CA2 field is a region where there is an overlap of components from CA2 and CA1 (and perhaps CA3) and that the smaller cells are simply ectopic CA1 neurons. We cannot dismiss the possibility, however, that the smaller neurons are a distinctive subset of CA2 cells rather than CA1 neurons. At this point, there is no feature of the small CA2 neurons that we could detect that would distinguish them from the larger population of CA1 pyramidal cells. This issue remains open to further study and may be resolved

when more is known about the axonal trajectories of the small CA2/ectopic CA1 neurons.

### CA1 pyramidal cells are a much more homogeneous population than the CA3 cells

One of the most striking features of the CA1 pyramidal cell was its homogeneity of appearance throughout the field. The total dendritic length of our population of CA1 neurons was nearly 13.5 mm with a standard deviation of only 1 mm. We observed CA1 neurons with 1–3 primary apical dendrites. Those with the greater number of apical primary dendrites tended to have a somewhat longer total dendritic tree. But even here, concomitant decreases in the basal dendritic tree tended to normalize the total dendritic lengths of the cells. The CA1 cells had a slightly smaller mean dendritic length than the distal CA3 and CA2 pyramidal cells and about the same size as the mid CA3 cells. The configuration of the dendritic tree of the CA1 neurons was quite distinct from that of the CA3/CA2 neurons. The most notable differences occurred in stratum radiatum and stratum lacunosum-moleculare. In stratum radiatum, dendritic side branches were observed throughout the full depth of the layer. There was no evidence of decreased branches in the superficial one fifth of the layer which constituted the projection zone of the CA3/CA2 fields. In stratum lacunosum-moleculare, the CA1 dendrites tended to have a more wavy or oblique orientation whereas those in CA3 tended to be more linear and vertically oriented. The CA1 dendritic tree in stratum lacunosum-moleculare also tended to be wider in the transverse plane than in the septotemporal plane whereas in CA3, the apical tree had approximately equal dimensions in both planes.

### Conclusions

There has been increasing evidence to support the notion that neuronal dendrites and their spines undergo substantial modification in the mature animal (Purves et al., 1986). A number of studies have indicated that both the length of the dendritic tree and the number of spines can increase or decrease depending on environmental experience or brain pathology. The number, shape and size of hippocampal spines have also been observed to change in response to physiologically induced synaptic enhancement, (Desmond and Levy, 1986; Geinisman et al., 1991), to the hormonal state of the animal (Wooley and McEwen, 1993; Watanabe et al., 1992), or as a consequence of aging (Geinisman et al., 1992a, b). It will be of substantial interest to determine whether the overall shape or size of the hippocampal pyramidal cell dendritic tree varies with learning or some other facet of the behavioral state of the animal. The ability to carry out these latter studies will be dependent on the validity of the quantitative dendritic measurements that are carried out. We have demonstrated that the use of intracellular staining techniques in the thick *in vitro* hippocampal slice coupled with computer-aided analysis of the dendritic tree produces reliable estimates of the dendritic organization of hippocampal pyramidal cells. Cells in the CA1 region, which demonstrate robust and long lasting synaptic plasticity (Malenka and Nicoll, 1993), appear to have relatively stereotypical dendritic trees. It would be of interest, therefore, to employ techniques similar to those used in the present study to determine whether environmental experience, such as extensive learning and memory testing, might appreciably modify the structure of the CA1

pyramidal cells. For such an undertaking, the results of the present study constitute important baseline information.

### ACKNOWLEDGMENTS

This work was supported, in part, by NIH Grant NS 16980 to WMC and DGA and by a Grant-in-Aid for Scientific Research on Priority Areas No. 03251209 from the Ministry of Education, Science and Culture of Japan to NI.

### AVAILABILITY OF NEURONAL DATABASE

The neurons described in this study were analyzed with the Eutectics Neuron Tracing System. The authors will make available the data files for further scientific analysis of these neurons in Eutectics and/or ASCII formats on MS-DOS disks. Interested researchers should communicate with the corresponding author. E-Mail address: DAMARAL@CCMAIL.SUNYSB.EDU.

### LITERATURE CITED

- Amaral, D.G., and J.A. Dent (1981) Development of the mossy fibers of the dentate gyrus: I. A light and electron microscopic study of the mossy fibers and their expansions. *J. Comp. Neurol.* 195:51–86.
- Bilkey, D.K., and P.A. Schwartzkroin (1990) Variation in electrophysiology and morphology of hippocampal CA3 pyramidal cells. *Brain Res.* 514:77–83.
- Capowski, J.J., and M.J. Sedivec (1981) Accurate computer reconstruction and graphics display of complex neurons utilizing state-of-the-art interactive techniques. *Comput. Biomed. Res.* 14:518–532.
- Claiborne, B.J., D.G. Amaral, and W.M. Cowan (1986) A light and electron microscopic analysis of the mossy fibers of the rat dentate gyrus. *J. Comp. Neurol.* 246:435–458.
- Claiborne, B.J., D.G. Amaral, and W.M. Cowan (1990) Quantitative, three-dimensional analysis of granule cell dendrites in the rat dentate gyrus. *J. Comp. Neurol.* 302:206–219.
- Desmond, N.L., and W.B. Levy (1982) A quantitative anatomical study of the granule cell dendritic field of the rat dentate gyrus using novel probabilistic method. *J. Comp. Neurol.* 212:131–145.
- Desmond, N.L., and W.B. Levy (1986) Changes in the numerical density of synaptic contacts with long-term potentiation in the hippocampal dentate gyrus. *J. Comp. Neurol.* 253:466–475.
- Fitch, J.M., J.M. Juraska, and L.W. Washington (1989) The dendritic morphology of pyramidal neurons in the rat hippocampal CA3 area. I. Cell types. *Brain Res.* 479:105–114.
- Geinisman, Y., L. deToledo-Morrell, and F. Morrell (1991) Induction of long-term potentiation is associated with an increase in the number of axospinous synapses with segmented postsynaptic densities. *Brain Res.* 566:77–88.
- Geinisman, Y., L. deToledo-Morrell, F. Morrell, I.S. Persina, and M. Rossi (1992a) Age-related loss of axospinous synapses formed by two afferent systems in the rat dentate gyrus as revealed by the unbiased stereological dissector technique. *Hippocampus* 2:437–444.
- Geinisman, Y., L. deToledo-Morrell, F. Morrell, I.S. Persina, and M. Rossi (1992b) Structural synaptic plasticity associated with the induction of long-term potentiation is preserved in the dentate gyrus of aged rats. *Hippocampus* 2:445–456.
- Golgi, C. (1886) *Sulla fina anatomia degli organi centrali del sistema nervoso*. Milan: Hoepli.
- Grace, A.A., and R. Llinás (1985) Morphological artifacts induced in intracellularly stained neurons by dehydration: circumvention using rapid dimethyl sulfoxide clearing. *Neuroscience* 16:461–475.
- Haglund, L., L.W. Swanson, and C. Köhler (1984) The projection of the supramammillary nucleus to the hippocampal formation: an immunohistochemical and anterograde transport study with the lectin PHA-L in the rat. *J. Comp. Neurol.* 229:171–185.
- Haschke, A., W. Mende, and H.G. Minkwitz (1980) Zur Entwicklung von Dendritenstrukturen an CA1-Pyramidenneuronen des Hippocampus der Ratte in Abhängigkeit ihrer Schichtenzugehörigkeit mit und ohne

- unspezifischer experimenteller Beeinflussung. Z. mikrosk.-anat. Forsch. (Leipzig) 4:593–622.
- Ishizuka, N., J. Weber, and D.G. Amaral (1990) Organization of intrahippocampal projections originating from CA3 pyramidal cells in the rat. *J. Comp. Neurol.* 295:580–623.
- Li, X-G, P. Somogyi, A. Ylinen, and G. Buzsaki (1994) The hippocampal CA3 network: an in vivo intracellular labeling study. *J. Comp. Neurol.* 339:181–208.
- Lorente de Nó, R. (1934) Studies on the structure of the cerebral cortex II. Continuation of the study of the ammonic system. *J. Psychol. Neurol.* (Leipzig) 46:113–117.
- Malenka, R.C., and R.A. Nicoll (1993) NMDA-receptor-dependent synaptic plasticity: multiple forms and mechanisms. *Trends Neurosci.* 1993 16:521–527.
- Masukawa, L.M., L.S. Benardo, and D.A. Prince (1982). Variations in electrophysiological properties of hippocampal neurons in different subfields. *Brain Research*, 242:341–344.
- McMullen, P.A., J.A. Saint-Cyr, and P.L. Carlen (1984) Morphological alterations in rat CA1 hippocampal pyramidal cell dendrites resulting from chronic ethanol consumption and withdrawal. *J. Comp. Neurol.* 225:111–118.
- Minkwitz, H.G. (1976a) Zur Entwicklung der Neuronenstruktur des Hippocampus während der prä- und postnatalen Ontogenese der Albinoratte. I. Mitteilung: Neurohistologische Darstellung der Entwicklung langaxoniger Neurone aus den Regionen CA3 und CA4. *Journal für Hirnforschung*, 17:213–231.
- Minkwitz, H.G. (1976b) Zur Entwicklung der Neuronenstruktur des Hippocampus während der prä- und postnatalen Ontogenese der Albinoratte. II. Mitteilung: Neurohistologische Darstellung der Entwicklung von Interneuronen und des Zusammenhangs lang- und kurzaxoniger Neurone. *Journal für Hirnforschung*, 17:233–253.
- Minkwitz, H.G. (1976c) Zur Entwicklung der Neuronenstruktur des Hippocampus während der prä- und postnatalen Ontogenese der Albinoratte. III. Mitt: Morphometrische Erfassung der ontogenetischen Veränderungen in Dendritenstruktur und Spinebesatz. *Journal für Hirnforschung*, 17:255–275.
- Pokorny, J., and T. Yamamoto (1981) Postnatal ontogenesis of hippocampal CA1 area in rats. I. Development of dendritic arborization in pyramidal neurons. *Brain Res. Bull.* 7:113–120.
- Purves, D., R.D. Hadley, and J.T. Voyvodic (1986) Dynamic changes in the dendritic geometry of individual neurons visualized over periods of up to three months in the superior cervical ganglion of living mice. *J. Neurosci.* 6:1051–1060.
- Ramón y Cajal, S. (1911) *Histologie du système nerveux de l'homme et des vertébrés. Tome II Maloine, Paris.*
- Sik, A., N. Tamamaki, and T.F. Freund (1993) Complete axon arborization of a single CA3 pyramidal cell in the rat hippocampus, and its relationship with postsynaptic parvalbumin-containing interneurons. *Eur. J. Neurosci.* 5:1719–1728.
- Steward, O., and S.A. Scoville (1976) Cells of origin of entorhinal cortical afferents to the hippocampus and fascia dentata of the rat. *J. Comp. Neurol.* 169:347–370.
- Tamamaki, N., and Y. Nojo (1993) Projection of the entorhinal layer II neurons in the rat as revealed by intracellular pressure-injection of neurobiotin. *Hippocampus* 3:471–480.
- Trommald, M., V. Jensen and P. Andersen (1995) Analysis of dendritic spines in rat CA1 pyramidal cells intracellularly filled with a fluorescent dye. *J. Comp. Neurol.* 353:260–274.
- Turner, D.A., and P.A. Schwartzkroin (1980) Steady-state electrotonic analysis of intracellularly stained hippocampal neurons. *J. Neurophysiol.* 44:184–199.
- Turner, D.A., and P.A. Schwartzkroin (1983) Electrical characteristics of dendrites and dendritic spines in intracellularly stained CA3 and dentate hippocampal neurons. *Journal of Neuroscience*, 3:2381–2394.
- Watanabe, Y., E. Gould, H.A. Cameron, D.C. Daniels, and B.S. McEwen (1992) Phenytoin prevents stress- and corticosterone-induced atrophy of CA3 pyramidal neurons. *Hippocampus* 2:431–435.
- West, J.R., C.A. Hodges, and J.A.C. Black (1981) Distal infrapyramidal granule cell axons possess typical mossy fiber morphology. *Brain Res. Bull.* 6:119–124.
- Woodhams, P.L., M.R. Celio, N. Ulfh, and M.P. Witter (1993) Morphological and functional correlates of borders in the entorhinal cortex and hippocampus. *Hippocampus Special Issue* 303–311.
- Woolley, C.S., and B.S. McEwen (1993) Roles of estradiol and progesterone in regulation of hippocampal dendritic spine density during the estrous cycle in the rat. *J Comp. Neurol.* 336:293–306.